

# Boundary Spectrum in the sine-Gordon Model with Dirichlet Boundary Conditions

Peter Mattsson<sup>1</sup> and Patrick Dorey<sup>2</sup>

*Dept. of Mathematical Sciences, University of Durham, Durham DH1 3LE, UK*

## Abstract

We find the spectrum of boundary bound states for the sine-Gordon model with Dirichlet boundary conditions, closing the bootstrap and providing a complete description of all the poles in the boundary reflection factors. The boundary Coleman-Thun mechanism plays an important role in the analysis. Two basic lemmas are introduced which should hold for any 1+1-dimensional boundary field theory, allowing the general method to be applied to other models.

## 1 Introduction

Integrable quantum field theories in two dimensions can be restricted from the whole line by certain boundary conditions while still preserving their integrability [1]. As well as being of theoretical interest, these models have interesting physical applications, for example to impurity problems in an interacting 1D electron gas [2] or edge excitations in fractional quantum Hall states [3, 4]. (A recent review can be found in [5].)

One such theory is the sine-Gordon model, which has the bulk action

$$\mathcal{A}_{SG} = \int_{-\infty}^{\infty} dx \int_{-\infty}^{\infty} dt \frac{1}{2} (\partial_{\mu} \varphi)^2 - \frac{m_0^2}{\beta^2} (\cos(\beta \varphi) - 1) \quad (1)$$

on the full line, where  $\varphi(x, t)$  is a scalar field and  $\beta$  is a dimensionless coupling constant. It was argued in [1] that this could be restricted to the half line  $x \in (-\infty, 0]$  while still preserving integrability by adding a “boundary action” term

$$- \int_{-\infty}^{\infty} dt M \cos \left[ \frac{\beta}{2} (\varphi_B - \varphi_0) \right], \quad (2)$$

where  $M$  and  $\varphi_0$  are free parameters, and  $\varphi_B(t) = \varphi(x, t)|_{x=0}$ . In addition to the usual bulk bound states, in general this also presents us with a complicated spectrum of boundary bound states. This aspect was mentioned briefly in [1, 6], and investigated in more detail in [7]. However in none of these works was a full explanation of all poles achieved. In this paper we return to the problem, and find that the full story appears to involve a much richer structure of boundary bound states than has previously been suggested. An important feature of our analysis, not taken into account in the earlier works, is the so-called boundary Coleman-Thun mechanism [8]. After a brief description of the boundary sine-Gordon model in section 2, this mechanism is reviewed in section 3. In the course of the section we also develop a couple of useful lemmas, which simplify the subsequent discussions considerably.

We will restrict ourselves to the case of Dirichlet boundary conditions, which simply fixes the value of the field at the boundary to  $\varphi(x=0, t) = \varphi_0$  for all time. This corresponds to taking  $M \rightarrow \infty$  above. After an initial discussion in section 4, in section 5 we make a complete analysis of a particular example. This serves to show many of the features of the bound state structure, and is a useful warm-up to the discussion of the general case in section 6. Finally, we gather together our conclusions in section 7.

<sup>1</sup>E-mail: P.A.Mattsson@dur.ac.uk

<sup>2</sup>E-mail: P.E.Dorey@dur.ac.uk

## 2 The reflection factors

### 2.1 The theory in the bulk

We begin with a summary of the theory in the bulk, mainly to set up the notation. Further details can be found in the review [9]. The bulk sine-Gordon model is known to be integrable at both the classical and the quantum levels [10]. The theory has an infinite number of degenerate vacua, with the discrete symmetry  $\varphi \rightarrow \varphi + \frac{2\pi}{\beta}m$ , with  $m \in \mathbb{Z}$ . The particle spectrum consists of a soliton ( $A$ ) and an anti-soliton ( $\bar{A}$ ) — both of which interpolate between neighbouring vacua — and a number of soliton – anti-soliton bound states (“breathers”)  $B_n$ ,  $n = 1, 2, \dots, < \lambda$ , where

$$\lambda = \frac{8\pi}{\beta^2} - 1. \quad (3)$$

The soliton (anti-soliton) has a topological charge of 1 (-1) while the breathers are neutral. The soliton and anti-soliton both have the same mass, which we shall call  $m_s$ , while the mass of the  $n^{\text{th}}$  breather  $B_n$  is  $m_n = 2m_s \sin\left(\frac{n\pi}{2\lambda}\right)$ .

The integrability of the theory means that particle production is forbidden, and all scattering is factorisable – the amplitude for any scattering process can be reduced to a product of two-particle amplitudes. In addition, charge, parity and time-reversal (C, P and T) symmetry holds for the bulk theory. If we denote the soliton S-matrix as  $S_{cd}^{ab}(\theta)$  for rapidity  $\theta$ , with  $a, b, c, d$  taking the value + (–) if the particle is a soliton (anti-soliton), the non-zero scattering amplitudes are  $S_{++}^{++}(\theta) = S_{--}^{--}(\theta) = a(\theta)$  (soliton-soliton or anti-soliton-anti-soliton scattering),  $S_{+-}^{+-}(\theta) = S_{-+}^{-+}(\theta) = b(\theta)$  (soliton-anti-soliton transmission), and  $S_{+-}^{+-}(\theta) = S_{-+}^{-+}(\theta) = c(\theta)$  (soliton-anti-soliton reflection). Explicitly,

$$\begin{aligned} a(\theta) &= \sin[\lambda(\pi - u)]\rho(u), \\ b(\theta) &= \sin(\lambda u)\rho(u), \\ c(\theta) &= \sin(\lambda\pi)\rho(u), \end{aligned} \quad (4)$$

where  $u = -i\theta$  and

$$\rho(u) = \frac{1}{\sin(\lambda(u - \pi))} \prod_{l=1}^{\infty} \left[ \frac{\Gamma((2l-2)\lambda - \frac{\lambda u}{\pi}) \Gamma(1 + 2l\lambda - \frac{\lambda u}{\pi})}{\Gamma((2l-1)\lambda - \frac{\lambda u}{\pi}) \Gamma(1 + (2l-1)\lambda - \frac{\lambda u}{\pi})} / (u \rightarrow -u) \right]. \quad (5)$$

As pointed out in [11], this factor can also be written in terms of Barnes’ diperiodic sine function  $S_2(x|\omega_1, \omega_2)$  [12, 13]. This is a meromorphic function parametrised by the pair of ‘quasiperiods’  $(\omega_1, \omega_2)$ , with poles and zeroes at the following points:

$$\begin{aligned} \text{poles} &: x = n_1 \omega_1 + n_2 \omega_2 \quad (n_1, n_2 = 1, 2, \dots) \\ \text{zeroes} &: x = m_1 \omega_1 + m_2 \omega_2 \quad (m_1, m_2 = 0, -1, -2, \dots) \end{aligned} \quad (6)$$

In terms of this function,

$$\rho(u) = \frac{1}{\sin(\lambda(u - \pi))} \frac{S_2\left(\pi - u \middle| \frac{\pi}{\lambda}, 2\pi\right) S_2\left(u \middle| \frac{\pi}{\lambda}, 2\pi\right)}{S_2\left(\pi + u \middle| \frac{\pi}{\lambda}, 2\pi\right) S_2\left(-u \middle| \frac{\pi}{\lambda}, 2\pi\right)}. \quad (7)$$

The amplitudes  $b(\theta)$  and  $c(\theta)$  have simple poles at  $\theta = i\left(\pi - \frac{n\pi}{\lambda}\right)$ ,  $n = 1, 2, \dots, < \lambda$ , which can be attributed to the creation of  $B_n$  in the forward channel. There are also poles at  $\theta = \frac{i\pi n}{\lambda}$  in  $a(\theta)$  and  $b(\theta)$  corresponding to the same process in the cross channel. Since all poles that we will be discussing, both in the bulk and at the boundary, occur at imaginary rapidities, from now on we will use the variable  $u = -i\theta$  and always work in terms of purely imaginary rapidities.

### 2.2 Solitonic ground state reflection factors

The general integral boundary condition found in [1] does not conserve topological charge, so in principle four solitonic boundary reflection factors need to be introduced, as well as a set of breather reflection factors. The solitonic factors which we quote here were given in [1], while breather factors can be found in [6].

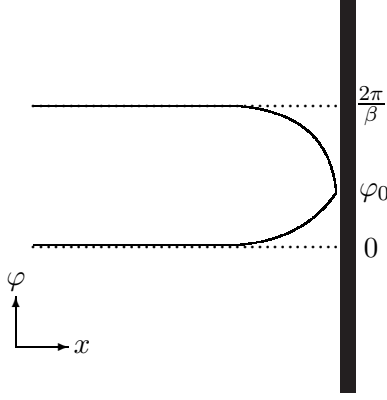


**Figure 1: Vacuum structure**

The reflection factors for the sine-Gordon solitons off the boundary ground state will be denoted by  $P_{\pm}(u)$  (a soliton or anti-soliton, incident on the boundary, is reflected back unchanged) and  $Q_{\pm}(u)$  (a soliton is reflected back as an anti-soliton, or vice versa). In the Dirichlet case, topological charge is conserved and so  $Q_{\pm} = 0$ . The remaining factors can be written as<sup>3</sup>

$$P^{\pm}(u) = R_0(u) \prod_{l=1}^{\infty} \left[ \frac{\Gamma\left(\frac{1}{2} + 2l\lambda \pm \frac{\xi}{\pi} + \frac{\lambda u}{\pi}\right) \Gamma\left(\frac{1}{2} + (2l-2)\lambda \mp \frac{\xi}{\pi} + \frac{\lambda u}{\pi}\right)}{\Gamma\left(\frac{1}{2} + (2l-1)\lambda + \frac{\xi}{\pi} + \frac{\lambda u}{\pi}\right) \Gamma\left(\frac{1}{2} + (2l-1)\lambda - \frac{\xi}{\pi} + \frac{\lambda u}{\pi}\right)} / (u \rightarrow -u) \right], \quad (8)$$

where

$$R_0(u) = \prod_{k=1}^{\infty} \left[ \frac{\Gamma\left(1 + \lambda(4k-4) - \frac{2\lambda u}{\pi}\right) \Gamma\left(4\lambda k - \frac{2\lambda u}{\pi}\right)}{\Gamma\left(\lambda(4k-3) - \frac{2\lambda u}{\pi}\right) \Gamma\left(1 + \lambda(4k-1) - \frac{2\lambda u}{\pi}\right)} / (u \rightarrow -u) \right], \quad (9)$$

and  $\xi = \frac{4\pi\varphi_0}{\beta}$ . These factors can again be written in terms of Barnes' multi-periodic functions, as

$$P^{\pm}(u) = R_0(u) \frac{S_2\left(\frac{\pi}{2\lambda} \mp \frac{\xi}{\lambda} + \pi + u \mid \frac{\pi}{\lambda}, 2\pi\right) S_2\left(\frac{\pi}{2\lambda} \mp \frac{\xi}{\lambda} - u \mid \frac{\pi}{\lambda}, 2\pi\right)}{S_2\left(\frac{\pi}{2\lambda} \mp \frac{\xi}{\lambda} + \pi - u \mid \frac{\pi}{\lambda}, 2\pi\right) S_2\left(\frac{\pi}{2\lambda} \mp \frac{\xi}{\lambda} + u \mid \frac{\pi}{\lambda}, 2\pi\right)}, \quad (10)$$

with

$$R_0(u) = \frac{S_2\left(\frac{\pi}{2} - u \mid \frac{\pi}{2\lambda}, 2\pi\right) S_2\left(\frac{\pi}{2\lambda} + u \mid \frac{\pi}{2\lambda}, 2\pi\right)}{S_2\left(\frac{\pi}{2} + u \mid \frac{\pi}{2\lambda}, 2\pi\right) S_2\left(\frac{\pi}{2\lambda} - u \mid \frac{\pi}{2\lambda}, 2\pi\right)}. \quad (11)$$

The theory is invariant under  $\varphi_0 \rightarrow \varphi_0 + \frac{2\pi}{\beta}$ , and also under the simultaneous transformations  $\varphi_0 \rightarrow -\varphi_0$  and soliton  $\rightarrow$  anti-soliton. Introducing the boundary breaks the degeneracy of the bulk vacua, and selects the lower line in figure 1 as the lowest-energy state, with the upper line as the first excited state. Continuing  $\varphi_0$  through  $\frac{\pi}{\beta}$  thus simply interchanges the rôles of these two states, and selects the upper one as the ground state.

In light of this, we are free to choose  $\xi$  to be in the interval

$$0 < \xi < \frac{4\pi^2}{\beta^2} = \frac{\pi(\lambda+1)}{2}. \quad (12)$$

Note that the topological charge of the ground state is no longer zero, as in the bulk model, but

$$q = \frac{\beta}{2\pi} \int_{-\infty}^0 dx \frac{\partial}{\partial x} \varphi(x, t) = \frac{\beta}{2\pi} [\varphi(0, t) - \varphi(-\infty, t)] = \frac{\beta\varphi_0}{2\pi}, \quad (13)$$

with the charge of the first excited state being  $1 - \frac{\beta\varphi_0}{2\pi}$ . We will find that all the boundary states have one of these charges so, for convenience, we shall designate them simply as 0 and 1 respectively.

<sup>3</sup>Note that there is a small error in Ghoshal and Zamolodchikov's formula (5.23) for  $\sigma$ , where the denominator should read  $\Pi(x, \pi/2)\Pi(-x, \pi/2)\Pi(x, -\pi/2)\Pi(-x, -\pi/2)$ . We are grateful to Subir Ghoshal for informing us of the corrected version.

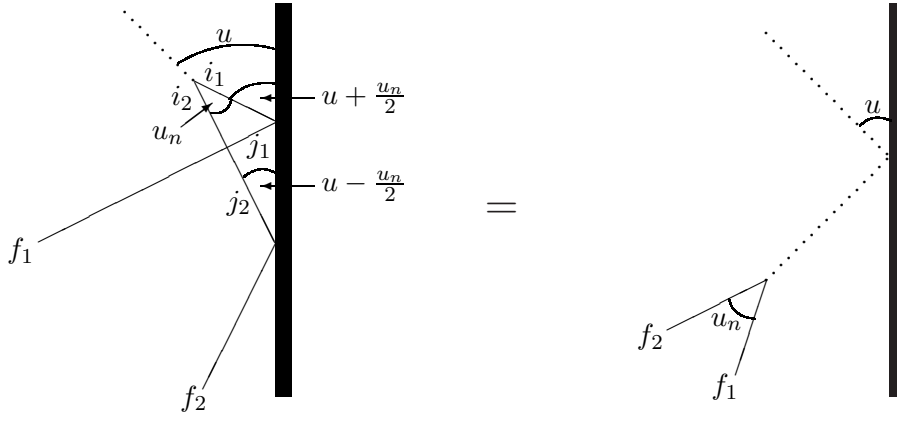


**Figure 2: Breather bootstrap**

### 2.3 Breather ground state reflection factors

For the breather sector, Ghoshal [6] obtained the relevant reflection factors —  $R_{|0\rangle}^n(u)$  for breather  $n$  and boundary ground state  $|0\rangle$  — from the solitonic reflection factors using the general boundary bootstrap equation [14, 1]

$$f_{i_1 i_2}^n R_{j_1 |x\rangle}^{i_1} \left(u + \frac{u_n}{2}\right) S_{j_2 f_1}^{i_2 j_1}(2u) R_{f_2 |x\rangle}^{j_2} \left(u - \frac{u_n}{2}\right) = f_{f_1 f_2}^n R_{|x\rangle}^n(u), \quad (14)$$

where  $u_n = \pi - \frac{n\pi}{\lambda}$ , and the  $R_{b|x\rangle}^a(u)$  are the solitonic reflection factors, such that  $R_{-|x\rangle}^+(u)$  is the factor for a soliton to be reflected back as an anti-soliton and so on. The  $f_{ab}^n$  are the bulk vertices for the creation of breather  $n$  from (anti-)solitons  $a$  and  $b$ . These obey  $f_{+-}^n = (-1)^n f_{-+}^n$ . The bootstrap is illustrated in figure 2.

In the Dirichlet case, with topological charge conserved, the bootstrap equation reduces to

$$f_{i_1 i_2}^n P_{|x\rangle}^{i_1} \left(u + \frac{u_n}{2}\right) S_{f_2 f_1}^{i_2 i_1}(2u) P_{|x\rangle}^{f_2} \left(u - \frac{u_n}{2}\right) = f_{f_1 f_2}^n R_{|x\rangle}^n(u). \quad (15)$$

Ghoshal found that, for the boundary ground state, the breather reflection factors were

$$R_{|0\rangle}^n(u) = R_0^{(n)}(u) R_1^{(n)}(u), \quad (16)$$

where

$$R_0^{(n)}(u) = \frac{\left(\frac{1}{2}\right) \left(\frac{n}{2\lambda} + 1\right)}{\left(\frac{n}{2\lambda} + \frac{3}{2}\right)} \prod_{l=1}^{n-1} \frac{\left(\frac{l}{2\lambda}\right) \left(\frac{l}{2\lambda} + 1\right)}{\left(\frac{l}{2\lambda} + \frac{3}{2}\right)^2}, \quad (17)$$

and

$$R_1^{(n)}(u) = \prod_{l=\frac{1-n}{2}}^{\frac{n-1}{2}} \frac{\left(\frac{\xi}{\lambda\pi} - \frac{1}{2} + \frac{l}{\lambda}\right)}{\left(\frac{\xi}{\lambda\pi} + \frac{1}{2} + \frac{l}{\lambda}\right)}. \quad (18)$$

This makes use of the notation

$$(x) = \frac{\sinh\left(\frac{\theta}{2} + \frac{i\pi x}{2}\right)}{\sinh\left(\frac{\theta}{2} - \frac{i\pi x}{2}\right)}, \quad (19)$$

which will also be helpful later.

## 3 The boundary Coleman-Thun mechanism

In this section we will discuss some general features of the pole analysis of boundary reflection factors, in preparation for the specific case of the sine-Gordon model. The main aim is to establish a couple of lemmas which will simplify the subsequent discussion. We begin by recalling the story in the bulk.

An initially mysterious feature of the sine-Gordon S-matrix was the presence of a number of double poles in the breather scattering amplitudes. At first it was thought that these might be related to the integrability

of the model, and it was only with the work of Coleman and Thun [15] that it was realised that they had a ‘prosaic’ origin as anomalous threshold poles, and could be explained using standard field-theoretical ideas. Studies of affine Toda field theories [16, 17, 18, 19] returned to this topic, and it proved possible, in certain cases, to confirm the scenario of Coleman and Thun through standard, albeit elaborate, perturbative calculations [18].

One element of Coleman and Thun’s analysis was the observation that in 1+1 dimensions sometimes even simple poles have complicated explanations, as anomalous thresholds. This breaks the usual association of every simple S-matrix pole with a bound state in either the forward or the crossed channel. The same mechanism is at work in the S-matrices of non self-dual affine Toda field theories [19], as was pointed out in [20]. This material is reviewed at greater length in [21]; here, we are more interested in what can occur when a boundary is also involved. This was discussed in [8] via a particularly simple example, the boundary scaling Lee-Yang model, for which the spectrum of boundary bound states had previously been found by other means [22]. It was found that the Coleman-Thun mechanism did indeed play a role, there being a number of simple poles in the reflection factors at locations which did not correspond to boundary bound states, but which rather could be explained through on-shell (anomalous threshold) diagrams for multiple rescattering processes involving the boundary. Further work, applying the method to affine Toda field theories, can be found in [23]. It is important to remark that, both in the bulk and at the boundary, an anomalous threshold diagram would normally lead to a pole of order greater than one. To match a simple pole, this order must be reduced somehow, and in [8, 23] this was always achieved by one or more ‘internal’ reflection factors having zeroes exactly at the point where the diagram went on-shell. Here, we will see both this mechanism of order reduction (which mimics that seen in bulk affine Toda theories [20]) and cancellations between different diagrams, closer to the original situation discussed by Coleman and Thun [15].

One difficulty, especially serious in cases when the spectrum of boundary bound states is not known a priori, is the greatly increased complexity of the on-shell diagrams once a boundary is involved. This makes it hard to be sure that any given pole really does correspond to a new boundary bound state. In the bulk, a simple geometrical argument shows that poles in the S-matrix elements of the lightest particle can never be explained by a Coleman-Thun mechanism, and so must always be due to bound states [17]. We wish to find analogous criteria for the boundary situation. To this end, the following two lemmas turn out to be useful. Suppose the incoming particle is of type  $a$ , and that its reflection factor has a simple pole at  $\theta = iu$ .

**Lemma 1** *Let  $\overline{U}_a = \min_{b,c}(\pi - U_{ab}^c)$ . If  $u < \overline{U}_a$ , then the pole at  $iu$  cannot be explained by a Coleman-Thun mechanism, and so must correspond to the binding of particle  $a$  to the boundary, either before or after crossing the outgoing particle.*

**Proof:** All processes must take the form shown in figure 3 or the crossed version shown in figure 4. Conservation of momentum demands that all rescattering must take place within the hatched region, which is drawn from the furthest point from the boundary where either the incoming or outgoing particle undergoes any interaction. If neither particle decays, we simply have a diagram of the form of figure 8 or figure 9. Otherwise, momentum conservation requires that neither product of the particle which decays on the boundary of the hatched region has a trajectory which takes it outside that region. Fixing the notation by figure 6 (with angles  $U_{ac}^b$  and  $U_{ab}^c$  defined correspondingly), this reduces to demanding  $\pi - U_{ab}^c \leq u \leq U_{ac}^b$ . If we introduce  $\overline{U}_a$  then we must have  $\overline{U}_a \leq u \leq \pi - \overline{U}_a$  (i.e. just  $u \geq \overline{U}_a$ , as  $u \leq \frac{\pi}{2}$ ). Thus, if  $u < \overline{U}_a$ , then the only possible explanations for the pole are figure 8 and figure 9.

**Lemma 2** *If the boundary is in its ground state, then lemma 1 can be strengthened, requiring that the incoming particle bind to the boundary if  $u$  is outside the range  $\overline{U}_a < u < \frac{\pi}{2} - \overline{U}_a$ . In addition, if  $\min_{b,c} U_{bc}^a > \frac{\pi}{2}$ , the incoming particle must always bind to the boundary.*

**Proof:** With the boundary in its ground state, all rescattering must take place in the area shown in figure 5. Reasoning as before but demanding that both product particles be emitted into this more restricted region, we find  $\pi - U_{ab}^c \leq u \leq U_{ac}^b - \frac{\pi}{2}$ , or  $\overline{U}_a \leq u \leq \frac{\pi}{2} - \overline{U}_a$ . In addition, both particles  $b, c$  must be emitted into an angle of  $\frac{\pi}{2}$ , so  $U_{bc}^a < \frac{\pi}{2}$  for at least one pair of particles  $b, c$ . If either of these conditions are violated, then the incoming particle must bind to the boundary.

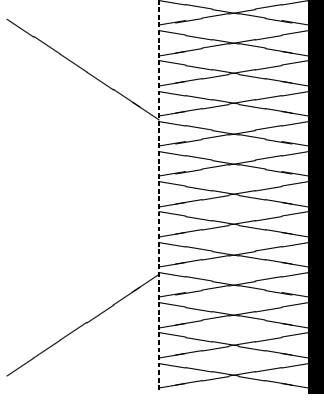


*Figure 3: General process, uncrossed*

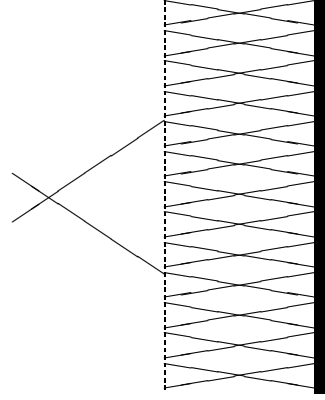


*Figure 4: General process, crossed*

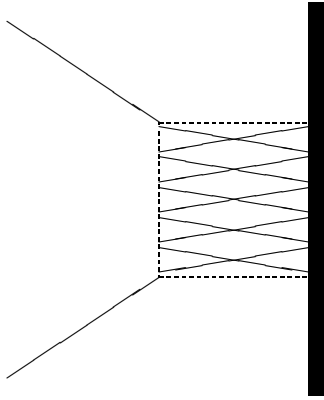


*Figure 5: General ground state process*

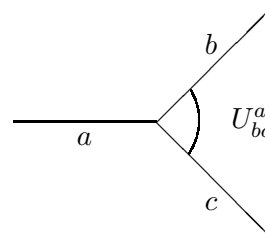


*Figure 6: Decay process*

These two results, between them, will allow the spectrum of the sine-Gordon model with Dirichlet boundary conditions to be fixed completely, provided it is assumed that no pole corresponds to the creation of a boundary state if it has an alternative (Coleman-Thun) explanation.

For the problem under discussion, writing the rapidity bounds  $\overline{U}_a$  as  $\overline{U}_{+(-)}$  for the soliton (anti-soliton) and as  $\overline{U}_n$  for the  $B_n$ , we have

$$\begin{aligned}\overline{U}_{\pm} &= \frac{\pi}{2} - \frac{n_{\max}\pi}{2\lambda} \\ \overline{U}_n &= \frac{\pi}{2\lambda}, \quad n \neq n_{\max} \\ \overline{U}_{n_{\max}} &= \frac{\pi}{2} - \frac{n_{\max}\pi}{2\lambda},\end{aligned}\tag{20}$$

where  $B_{n_{\max}}$  is the highest-numbered breather present in the model. To derive these results, note that a soliton (anti-soliton) can only decay into an anti-soliton (soliton) and a breather (with vertex  $U_{\mp n}^{\pm} = \frac{\pi}{2} + \frac{n\pi}{2\lambda}$ ). A breather can either decay into a soliton-anti-soliton pair ( $U_{+-}^n = \pi - \frac{n\pi}{\lambda}$ ) or a pair of breathers ( $U_{nm}^l = \pi - \frac{l\pi}{2\lambda}$  with  $n = m + l$  or  $m = n + l$ , or  $U_{nm}^l = \frac{\pi(n+m)}{2\lambda}$  with  $l = n + m$ ).

These restrictions can also be combined to produce a stronger version of lemma 1 when the incoming particle is a soliton. If  $\overline{U}_+ < u < \frac{\pi}{\lambda}$ , decay within the hatched region is only possible into the topmost breather and an anti-soliton. One or other of these particles will be heading away from the centre of the diagram. If the process is uncrossed, as in figure 3, the breather will be created heading towards the centre of the diagram, the anti-soliton away (we are being somewhat cavalier with the direction of time; this should be considered as a purely geometric argument). The anti-soliton must itself obey our lemmas; if in any further decay before it reaches the boundary one of the decay products is heading away from the boundary, then there would be no way to close the diagram while conserving momentum at every vertex. For a crossed process (figure 4) the breather is the outermost particle, and is again restricted in its decay by our lemmas for the same reason.

The anti-soliton created by the uncrossed process heads for the boundary with a rapidity less than  $\overline{U}_-$  and so, by lemma 1, may not decay. By the same token, the breather of the crossed process cannot decay either so, if the initial soliton is not to form a bound state, the only possible alternative processes are figure 18 and figure 19. If these are found not to occur (for example, if the necessary boundary vertices are not present) then the pole must correspond to a bound state for any  $u < \frac{\pi}{\lambda}$ .

## 4 Initial pole analysis

### 4.1 Solitonic ground state factors

The  $R_0(u)$  factor is insensitive to the boundary parameters, and so all its poles should be explicable in terms of the bulk. The only poles are at  $u = \frac{N\pi}{2\lambda}$ , where  $N = 1, 2, 3, \dots$ , with no zeroes. These can be explained by the creation of a breather which is incident perpendicularly on the boundary, as shown in figure 7. Here, as in all subsequent diagrams, the time axis points up the page, and the  $x$  axis points to the right. Solitons and anti-solitons are drawn as solid lines, while breathers are drawn as dotted lines.

Turning now to  $\xi$ -dependent poles and zeroes, we find zeroes at

$$u = -\frac{\xi}{\lambda} + \frac{(2n+1)\pi}{2\lambda},\tag{21}$$

where  $n = 0, 1, 2, \dots$ , for  $P^+$ , and at the same rapidities but with  $\xi \rightarrow -\xi$  for  $P^-$ . There are also poles in  $P^+$  only at  $u = \nu_n$ , with

$$\boxed{\nu_n = \frac{\xi}{\lambda} - \frac{(2n+1)\pi}{2\lambda}}\tag{22}$$

A soliton can only decay into an anti-soliton and a breather, with a rapidity difference between the two of  $\frac{\pi}{2} + \frac{b\pi}{2\lambda}$  for breather  $b$ . Thus, by lemma 2, all these poles must correspond to bound states, as shown in figure 8. For reasons which will become clear in a moment, we shall depart from the convention of [7] and, rather than labelling the state corresponding to pole  $\nu_n$  as  $\beta_n$ , will label it according to topological charge and  $n$  as  $|1; n\rangle$ .

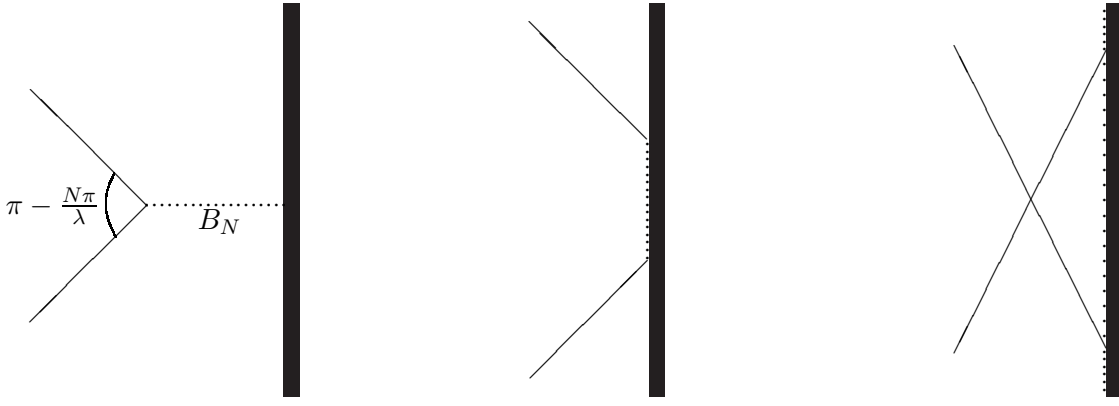


Figure 7:  $\xi$ -independent pole

Figure 8: Bound state

Figure 9: Crossed process

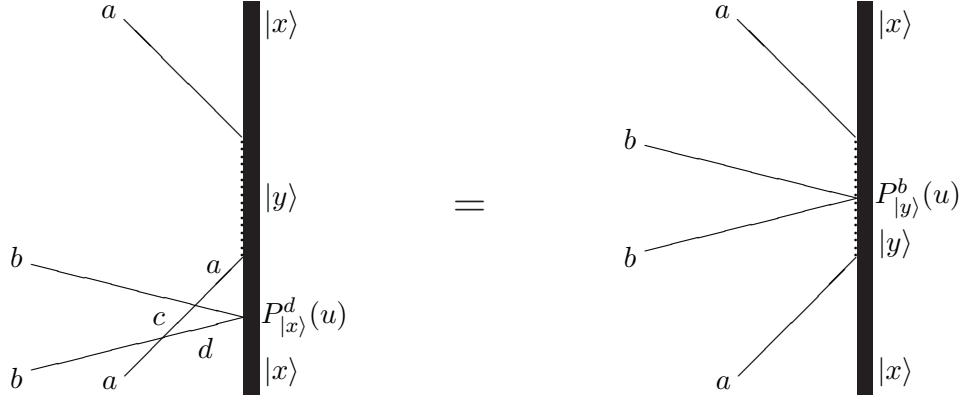


Figure 10: Boundary bound-state bootstrap

#### 4.2 Solitonic excited state reflection factors

Using the boundary bootstrap equations given in [1] — which come from considering figure 10 — solitonic reflection factors can be calculated for this first set of bound states. In our case, these equations read

$$P_{|y\rangle}^b(u) = \sum_{c,d} P_{|x\rangle}^d(u) S_{cd}^{ab}(u - \alpha_{ax}^y) S_{ba}^{dc}(u + \alpha_{ax}^y), \quad (23)$$

where  $a, b, c$ , and  $d$  take the values  $+$  or  $-$  and  $\alpha_{ax}^y$  is the (imaginary) rapidity of the pole at which particle  $a$  binds to boundary state  $|x\rangle$  to give state  $|y\rangle$ . The mass of state  $|y\rangle$  —  $m_y$  — is given by

$$m_y = m_x + m_s \cos \alpha_{ax}^y. \quad (24)$$

Taking  $x$  to be the ground state  $|0\rangle$  and  $y$  to be one of the set of excited states  $|1; n\rangle$ , this gives

$$\begin{aligned} P_{|1;n\rangle}^+(u) &= P_{|0\rangle}^+(u) a(u - \nu_n) a(u + \nu_n) \\ P_{|1;n\rangle}^-(u) &= P_{|0\rangle}^-(u) b(u - \nu_n) b(u + \nu_n) + P_{|0\rangle}^+(u) c(u - \nu_n) c(u + \nu_n). \end{aligned} \quad (25)$$

Note that  $P_{|1;0\rangle}^\pm(u) = \overline{P_{|0\rangle}^\mp(u)}$ , where  $\overline{P^\pm(u)}$  is  $P^\pm(u)$  under the transformation  $\xi \rightarrow \pi(\lambda + 1) - \xi$ . The reason for this is clear if we look back at figure 1; this transformation is equivalent to reflecting the diagram in the horizontal axis, interchanging the ground and first excited states.

Perhaps the neatest way to write the new reflection factors is

$$P_{|1;n\rangle}^\pm(u) = \overline{P^\mp(u)} a_n^1(u), \quad (26)$$



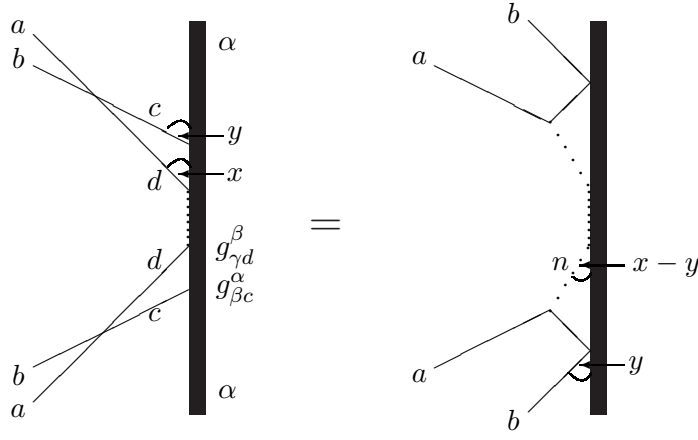


**Figure 11: States can be created either by breathers or solitons**

where

$$a_n^1(u) = \frac{a(u + \nu_n)a(u - \nu_n)}{a(u + \nu_0)a(u - \nu_0)}. \quad (27)$$

The factor  $a_n^1(u)$  simplifies to

$$a_n^1(u) = \prod_{x=1}^n \frac{\left(\frac{\xi}{\lambda\pi} + \frac{1}{2\lambda} - \frac{x}{\lambda}\right) \left(\frac{\xi}{\lambda\pi} - \frac{1}{2\lambda} - \frac{x}{\lambda}\right)}{\left(\frac{\xi}{\lambda\pi} + \frac{1}{2\lambda} - \frac{x}{\lambda} + 1\right) \left(\frac{\xi}{\lambda\pi} - \frac{1}{2\lambda} - \frac{x}{\lambda} + 1\right)}. \quad (28)$$

Looking at the pole structure, we find that the functions  $\overline{P^\pm(u)}$  have common simple poles at  $\nu_0$  and  $\nu_{-N}$  where  $N = 1, 2, 3, \dots$ . In addition,  $\overline{P^+}(u)$  has simple poles at  $u = w_{N'}$ , where

$$w_{N'} = \pi - \frac{\xi}{\lambda} - \frac{\pi(2N'-1)}{2\lambda} = \overline{\nu_{N'}} \quad (29)$$

and  $N' = 1, 2, 3, \dots$ , and simple zeroes at  $-w_{N''}$  for appropriate values of  $N''$ . Finally,  $a_n^1(u)$  has simple poles at  $\nu_0$  and  $\nu_n$ , and double poles at  $\nu_k$ ,  $k = 1, 2, \dots, n-1$ .

Before proceeding to a more rigorous discussion, we shall now digress to give an outline of how the bootstrap might be expected to work. If one of these poles *does* correspond to a new bound state, factorisability leads us to expect that moving the soliton and anti-soliton trajectories past each other (so that the anti-soliton is incident on the boundary first) should also create the same state. The most obvious explanation for this would be for the anti-soliton to bind to the boundary first, followed by the soliton, to form the state. From above, however, only solitons can bind to the ground state, so we must look further.

The *next* most obvious way this could happen is via the soliton and anti-soliton forming a breather, either before or after the anti-soliton has reflected from the boundary. The poles required to allow the first process (of the form  $\pi + \frac{\xi}{\lambda} - \frac{\pi(2m+1)}{2\lambda}$ ) are not present, whereas those necessary for the second (of the form  $w_m$ ) are. Our candidate process therefore becomes figure 11, where the soliton and anti-soliton bind to form a breather, which then creates the state in one step. It is quite difficult to imagine any further alternatives, so let us — for the moment — take the existence of such a process as a necessary condition for a pole to be responsible for the formation of a boundary state.

The consequence of this is that the  $w_N$  poles are selected as the only possible candidates, and it appears that new bound states can only be formed by anti-solitons. Such states hence have charge 0 (agreeing with the idea that they can also be formed from the ground state by the action of a breather). In addition, it is also clear that only those  $w_N$  such that  $w_N < \nu_n$  can be considered, as, otherwise, the breather version of the process would see the breather created heading away from the boundary, rather than towards it.

Designating such a new state as  $|0; n, N\rangle$  and bootstrapping on it leads to

$$\begin{aligned} P_{|0; n, N\rangle}^-(u) &= P_{|1; n\rangle}^-(u)a(u - w_N)a(u + w_N) \\ P_{|0; n, N\rangle}^+(u) &= P_{|1; n\rangle}^+(u)b(u - w_N)b(u + w_N) + P_{|1; n\rangle}^-(u)c(u - w_N)c(u + w_N). \end{aligned} \quad (30)$$

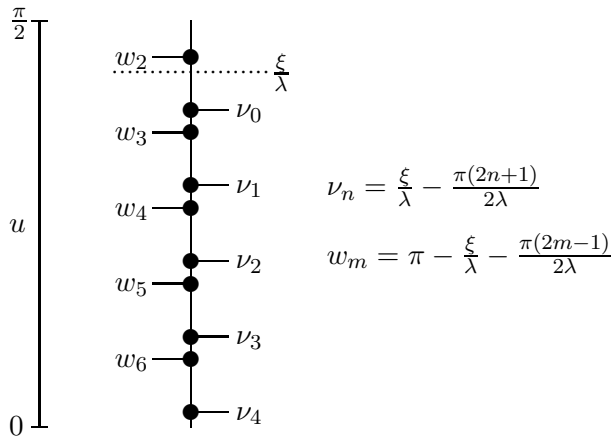


**Figure 12: Location of poles.** (Note that, in this case,  $w_2$  can never participate in bound state formation as it is above  $\nu_0$ .)

Substituting in (26) and taking advantage of the fact that  $w_N = \overline{\nu_N}$  (so  $a(u \pm w_N) = \overline{a(u \pm \nu_N)}$ ), this becomes

$$\begin{aligned} P_{|0;n,N\rangle}^-(u) &= a_n^1(u) \overline{P_{|0\rangle}^+(u)} a(u - \overline{\nu_N}) a(u + \overline{\nu_N}) \\ P_{|0;n,N\rangle}^+(u) &= a_n^1(u) \overline{P_{|0\rangle}^-(u)} b(u - \overline{\nu_N}) b(u + \overline{\nu_N}) + \overline{P_{|0\rangle}^+(u)} c(u - \overline{\nu_N}) c(u + \overline{\nu_N}), \end{aligned} \quad (31)$$

which (apart from an extra factor of  $a_n^1(u)$ ) is just the first bootstrap (25) under the transformation  $\xi \rightarrow \pi(\lambda + 1) - \xi$  and with solitons and anti-solitons interchanged on the lhs. Thus, the pole structure follows naturally from the above. This can also be written as

$$P_{|0;n,N\rangle}^\pm(u) = P_{|0\rangle}^\pm(u) a_n^1(u) \overline{a_N^1(u)}. \quad (32)$$

Repeating the factorisation argument shows that now we should focus on  $\nu_{n'}$  poles such that  $\nu_{n'} < w_N$ . These are present now in the solitonic factor, though (due to the extra factor of  $a_n^1(u)$ ) only for  $n' > n$ . However, since any such state obeys  $\nu_n > w_N > \nu_{n'}$  in any case, this restriction is not relevant. The resultant state must now have charge 0.

A pattern is emerging, and it is not hard to see how the process would continue. Starting from the ground state, and taking the broadest guess (given our assumptions) for the spectrum, states can be formed by alternating solitons and anti-solitons, the solitons having rapidity  $\nu_{n_i}$  and the anti-solitons having rapidity  $w_{N_j}$  (for some sets  $\underline{n}$  and  $\underline{N}$ ). An schematic pole structure is shown in figure 12, in terms of which the criterion for a state to be in the spectrum should be that we begin with one of the  $\nu_n$  and then, as we move along the index list, move down the diagram, switching from side to side as we go. If we finish on a  $\nu_m$  (indicating that the most recent particle to bind was a soliton) the state has charge 1 while, if we finish on a  $w_m$  (meaning an anti-soliton) the state has charge 0.

Annotating such a state by its topological charge,  $c$ , and the sets  $\underline{n}$  and  $\underline{N}$  as  $|c; n_1, N_1, n_2, N_2, \dots\rangle$  (noting  $\nu_{n_1} > w_{N_1} > \nu_{n_2} > w_{N_2} > \dots$ ), the solitonic reflection factors should be

$$P_{|c;n_1,N_1,\dots\rangle}^\pm(u) = P_{(c)}^\pm(u) a_{n_1}^1(u) \overline{a_{N_1}^1(u)} \dots, \quad (33)$$

with  $P_0^\pm(u) = P_{|0\rangle}^\pm(u)$  and  $P_1^\pm(u) = \overline{P_{|0\rangle}^\pm(u)}$ . From now on, however, it will be more convenient to consider a single index list, and denote  $\overline{a_m^1(u)}$  as  $a_m^0(u)$ , giving

$$P_{|c;n_1,n_2,\dots,n_k\rangle}^\pm(u) = P_{(c)}^\pm(u) a_{n_1}^1(u) a_{n_2}^0(u) a_{n_3}^1(u) \dots a_{n_k}^c(u), \quad (34)$$

where  $c$  is 1 if  $k$  is odd, and 0 if  $k$  is even. We will call this a level  $k$  boundary bound state. If we choose the ground state mass to be  $m_s \sin^2\left(\frac{\xi - \frac{\pi}{2}}{2\lambda}\right)$ , the mass of this state is

$$m_{n_1,n_2,\dots} = m_s \sin^2\left(\frac{\xi - \frac{\pi}{2}}{2\lambda}\right) + \sum_{i \text{ odd}} m_s \cos(\nu_{n_i}) + \sum_{j \text{ even}} m_s \cos(w_{n_j}) \quad (35)$$

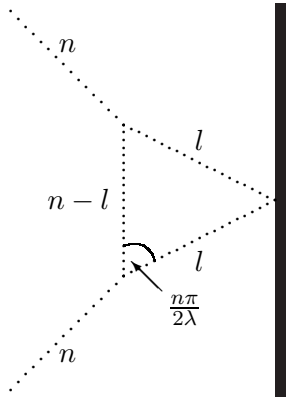


**Figure 13: Breather triangle process**

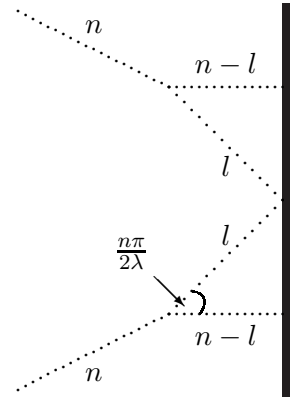


**Figure 14: Breather double triangle process**

$$= m_s \sin^2 \left( \frac{\xi - \frac{\pi}{2}}{2\lambda} \right) + \sum_{i \text{ odd}} m_s \cos \left( \frac{\xi}{\lambda} - \frac{(2n_i + 1)\pi}{2\lambda} \right) - \sum_{j \text{ even}} m_s \cos \left( \frac{\xi}{\lambda} + \frac{(2n_j - 1)\pi}{2\lambda} \right).$$

This choice is convenient in that, as  $\xi$  passes  $\pi/\beta$ , the masses of the ground and first excited states interchange, in line with the idea that the states themselves swap at this point. An important point to note is that, in deriving all this, we have simply been considering the soliton sector. However, we will see that allowing breather processes as well does not give rise to any further states, merely additional ways to jump between states. The Dirichlet boundary condition is also special in that either the soliton or the anti-soliton can couple to a given boundary, but not both, as might be generically expected.

Although we have built up the states by applying the solitons and anti-solitons in this alternating fashion, precisely how this happens in a given situation will of course depend on the impact parameters of the incoming particles. In figure 11 we already gave an example of the complicated way in which a process may be rearranged as these impact parameters vary, and the particular choices that we have adopted are mainly motivated by a desire to assemble the full spectrum in the simplest possible way.

### 4.3 Breather ground state reflection factors

We now return to the pole analysis, and examine the breather ground state reflection factors (16). Again, the factor  $R_0^n$  is boundary-independent, and so all its poles should have an explanation in terms of the bulk. There are (physical strip) poles at  $\frac{\pi}{2}$ ,  $\frac{l\pi}{2\lambda}$ ,  $\frac{\pi}{2} - \frac{n\pi}{2\lambda}$ , and double poles at  $\frac{\pi}{2} - \frac{l\pi}{2\lambda}$ , with  $l = 1, 2, \dots, n-1$ . There are no zeroes. The pole at  $\frac{\pi}{2}$  is simply due to the breather coupling perpendicularly to the boundary, while the poles at  $\frac{l\pi}{2\lambda}$  are explained by figure 13. Next, the pole at  $\frac{\pi}{2} - \frac{n\pi}{2\lambda}$  comes from a breather version of figure 7,  $B_{2n}$  being formed. Finally, the double poles at  $\frac{\pi}{2} - \frac{l\pi}{2\lambda}$  are due to figure 14.

Moving on to the boundary-dependent part, there are poles at

$$u = \frac{\xi}{\lambda} - \frac{\pi}{2} \pm \frac{l\pi}{2\lambda}, \quad (36)$$

and zeroes at

$$\begin{aligned} u &= -\frac{\xi}{\lambda} + \frac{\pi}{2} \pm \frac{l\pi}{2\lambda} \\ u &= \frac{\xi}{\lambda} + \frac{\pi}{2} \pm \frac{l\pi}{2\lambda}, \end{aligned} \quad (37)$$

where, for a breather  $n$ ,  $l = n-1, n-3, \dots, l \geq 0$ .

The set of poles can be re-written by noting that, for breather  $m$ , there is a simple pole of the form  $\frac{1}{2}(\nu_n - w_N)$  for all  $n, N \geq 0$  and  $n, N \in \mathbb{Z}$  such that  $m = n + N$ . This ties in with the discussion in the previous section, since these are the rapidities predicted for the single-step process which is equivalent to a soliton binding at an angle of  $\nu_n$  followed by an anti-soliton at  $w_N$ .

#### 4.4 Breather excited state reflection factors

Following the discussion of the solitonic excited state reflection factors, we can introduce corresponding breather reflection factors:

$$R_{|c;n_1,n_2,\dots,n_k\rangle}^m(u) = R_{(c)}^m(u) a_{n_1}^{1;m}(u) a_{n_2}^{0;m}(u) a_{n_3}^{1;m}(u) \dots a_{n_k}^{c;m}(u), \quad (38)$$

where  $R_0^m(u) = R_{|0\rangle}^m(u)$  and  $R_1^m(u) = \overline{R_{|0\rangle}^m(u)}$ . We have also defined

$$a_n^{c;m}(u) = a_n^c\left(u + \frac{u_m}{2}\right) a_n^c\left(u - \frac{u_m}{2}\right), \quad (39)$$

or

$$a_n^{1;m}(u) = \prod_{x=1}^m \frac{\left(\frac{\xi}{\lambda\pi} + \frac{1-2x-n}{2\lambda} + \frac{1}{2}\right) \left(\frac{\xi}{\lambda\pi} - \frac{1+2x+n}{2\lambda} + \frac{1}{2}\right) \left(\frac{\xi}{\lambda\pi} + \frac{1-2x+n}{2\lambda} - \frac{1}{2}\right) \left(\frac{\xi}{\lambda\pi} - \frac{1+2x-n}{2\lambda} - \frac{1}{2}\right)}{\left(\frac{\xi}{\lambda\pi} + \frac{1-2x-n}{2\lambda} - \frac{1}{2}\right) \left(\frac{\xi}{\lambda\pi} - \frac{1+2x+n}{2\lambda} - \frac{1}{2}\right) \left(\frac{\xi}{\lambda\pi} + \frac{1-2x+n}{2\lambda} + \frac{1}{2}\right) \left(\frac{\xi}{\lambda\pi} - \frac{1+2x-n}{2\lambda} + \frac{1}{2}\right)}, \quad (40)$$

with  $a_n^{0;m}(u) = \overline{a_n^{1;m}(u)}$ .

For  $\overline{R_{|0\rangle}^m(u)}$ , there are poles at

$$\begin{aligned} u &= \frac{\pi}{2} - \frac{\xi}{\lambda} + \frac{\pi}{\lambda} \pm \frac{l\pi}{2\lambda} \\ u &= \frac{\pi}{2} + \frac{\xi}{\lambda} - \frac{(l+2)\pi}{2\lambda}, \end{aligned} \quad (41)$$

and zeroes at

$$u = \frac{\xi}{\lambda} - \frac{\pi}{2} + \frac{(l-2)\pi}{2\lambda}. \quad (42)$$

For the other factors,  $a_n^{1;m}(u)$  has physical strip poles/zeroes at

$$\begin{aligned} u = -\frac{\xi}{\lambda} + \frac{\pi}{2} + \frac{p\pi}{2\lambda} & \quad \text{poles : } p = 2n - m + 2x \pm 1 \\ & \quad \text{zeroes : } p = -m + 2x \pm 1 \\ u = \frac{\xi}{\lambda} - \frac{\pi}{2} + \frac{p\pi}{2\lambda} & \quad \text{poles : } p = m - 2x \pm 1 \\ & \quad \text{zeroes : } p = -2n + m - 2x \pm 1 \\ u = \frac{\xi}{\lambda} + \frac{\pi}{2} + \frac{p\pi}{2\lambda} & \quad \text{poles : } p = -2n + m - 2x \pm 1 \\ & \quad \text{zeroes : } p = m - 2x \pm 1 \end{aligned} \quad (43)$$

while  $a_n^{0;m}(u)$  has them at

$$\begin{aligned} u = -\frac{\xi}{\lambda} + \frac{3\pi}{2} + \frac{p\pi}{2\lambda} & \quad \text{poles : } p = -2N - m + 2x \pm 1 \\ & \quad \text{zeroes : } - \\ u = -\frac{\xi}{\lambda} + \frac{\pi}{2} + \frac{p\pi}{2\lambda} & \quad \text{poles : } p = -m + 2x \pm 1 \\ & \quad \text{zeroes : } p = -2N - m + 2x \pm 1 \\ u = \frac{\xi}{\lambda} - \frac{\pi}{2} + \frac{p\pi}{2\lambda} & \quad \text{poles : } p = 2N + m - 2x \pm 1 \\ & \quad \text{zeroes : } p = m - 2x \pm 1 \\ u = \frac{\xi}{\lambda} + \frac{\pi}{2} + \frac{p\pi}{2\lambda} & \quad \text{poles : } p = m - 2x \pm 1 \\ & \quad \text{zeroes : } p = 2N + m - 2x \pm 1 \end{aligned} \quad (44)$$

These poles will be further discussed in section 6 below.

## 5 An example

To get an idea of the full picture, and which processes are responsible for the remaining poles, we will now look at one particular example in more detail. If we select  $\xi = 1.6\pi$  and  $\lambda = 2.5$ , then we have the first two breathers in the spectrum, with the solitonic poles taking the form  $\nu_n = \frac{\pi(2.2-2n)}{5}$  and  $w_N = \frac{\pi(2.8-2N)}{5}$ . Thus, for this case, only the poles at  $\nu_0, \nu_1$  and  $w_1$  are on the physical strip, and so figure 12 is simplified to figure 15. This is the simplest case which requires a broader spectrum than that postulated in [7]. First, let us turn to the soliton sector.

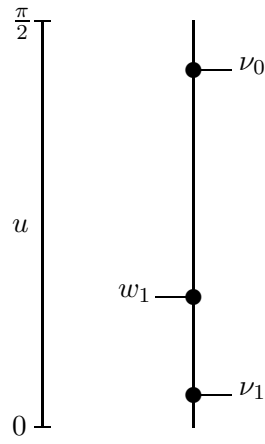


Figure 15: Location of poles in the example

### 5.1 Boundary ground state — soliton sector

As argued above, the soliton can bind to the boundary at all rapidities  $\nu_n$  which are in the physical strip, here just comprising  $\nu_0$  and  $\nu_1$ . This introduces the states  $|1;0\rangle$  and  $|1;1\rangle$ .

### 5.2 Boundary ground state — breather sector

The only breather poles are at  $\frac{\xi}{\lambda} - \frac{\pi}{2} + \frac{(m-1)\pi}{2\lambda}$  for breather  $m$ . In addition, breather  $B_2$  has a zero at  $-\frac{\xi}{\lambda} + \frac{\pi}{2} + \frac{\pi}{2\lambda}$ .

By lemma 1, the pole for  $B_1$  must correspond to a new bound state, the rapidity being less than  $\frac{\pi}{2\lambda}$ . From figure 11, it is clear that  $B_1$  creates the state which was labelled  $|\delta_{0,1}\rangle$  in [7], and which we have called  $|0;0,1\rangle$ .

The pole for the second breather can be explained by figure 21, with the state  $|1;0\rangle$  being formed. The anti-soliton is reflected from the boundary at a rapidity of  $\frac{\xi}{\lambda} - \pi + \frac{3\pi}{2\lambda}$  — a zero of the  $|1;0\rangle$  reflection factor — reducing the diagram to first order through the boundary Coleman-Thun mechanism.

### 5.3 First level excited states — soliton sector

From before,  $P_{|1;0\rangle}^+$  just has a simple pole at  $\nu_0$ , which can be explained by the crossed process in figure 9, reducing the boundary to the ground state. For  $P_{|1;1\rangle}^+$ , the pole at  $\nu_1$  can be explained this way while, for the double pole at  $\nu_0$ , figure 20 is required, the first breather being formed while the boundary is reduced to the vacuum state.

For  $P_{|1;n\rangle}^-(u)$ , we have the additional job of explaining simple poles at  $w_N$ , for all  $N$  such that this pole is in the physical strip. Here, this is only  $w_1$ . For  $|1;0\rangle$ , this is appropriate for the formation of  $|0;0,1\rangle$  which, from the previous section, must be present. For  $|1;1\rangle$ , however, figure 19 is invoked, the second breather being created, and the boundary reduced to the vacuum state. The breather is incident on the boundary at an angle of  $\frac{1}{2}(w_1 - \nu_1) = \pi - \frac{\xi}{\lambda} - \frac{\pi}{2\lambda}$  which, looking at the above breather reflection factors, is a zero, ensuring the diagram is of the correct order.

### 5.4 First level excited states — breather sector

The pole structure of  $R_{|1;0\rangle}^m$  can be found from  $\overline{R_{|0\rangle}^m}$ , and is

$$\begin{aligned} B_1 : & \text{ pole at } \frac{\pi}{2} - \frac{\xi}{\lambda} + \frac{\pi}{\lambda} \\ B_2 : & \text{ poles at } \frac{\pi}{2} - \frac{\xi}{\lambda} + \frac{3\pi}{2\lambda}, \frac{\pi}{2} - \frac{\xi}{\lambda} + \frac{\pi}{2\lambda} \end{aligned} \quad (45)$$

By lemma 1, the second pole for  $B_2$  must correspond to a new bound state; by the previous arguments, this is  $|1;0,1,1\rangle$ . This state is not in the spectrum given in [7], but lemma 1 shows that there is no way

to avoid its introduction. Considerations such as this will open the door to a much wider spectrum in the general case.

The  $B_1$  pole is suitable for the creation of  $|1;1\rangle$ . The first pole for  $B_2$  can be explained by figure 23, with the boundary being reduced to the ground state by emission of a soliton.

For  $R_{|1;1\rangle}^m$ , the above poles are supplemented by additional poles from  $a_1^{1;m}(u)$  to give the poles shown in table 1.

	$-\frac{\xi}{\lambda} + \frac{\pi}{2} + \frac{p\pi}{2\lambda}$	$\frac{\xi}{\lambda} - \frac{\pi}{2} + \frac{p\pi}{2\lambda}$	$\frac{\xi}{\lambda} + \frac{\pi}{2} + \frac{p\pi}{2\lambda}$
$B_1$	2	0	—
$B_2$	$3^2$	1	-5

**Table 1: Breather pole structure for  $|1;1\rangle$ .** Entries are the values of  $p$  for which there is a pole in the location given in the column heading. The power of the entry gives the order of the pole, so e.g.  $3^2$  indicates a double pole when  $p = 3$ . There are no physical strip zeroes for either breather.

The pole at  $\frac{\xi}{\lambda} + \frac{\pi}{2} - \frac{5\pi}{2\lambda}$  can be explained by figure 24, with the boundary being reduced to the ground state by emission of a soliton. The pole at  $\frac{\xi}{\lambda} - \frac{\pi}{2}$  for  $B_1$  can be allocated to the creation of  $|1;0,1,1\rangle$ , while the pole at  $\frac{\xi}{\lambda} - \frac{\pi}{2} + \frac{\pi}{2\lambda}$  for  $B_2$  is due to figure 25, where the boundary emits  $B_1$ , being reduced to  $|1;0\rangle$ . The pole at  $-\frac{\xi}{\lambda} + \frac{\pi}{2} + \frac{2\pi}{2\lambda}$  for  $B_1$  is responsible for this reduction to  $|1;0\rangle$ , while the double pole for  $B_2$  comes from an all-breather version of figure 22, the boundary being reduced in the same way.

### 5.5 Second level excited states — soliton sector

For  $P_{|0;0,1\rangle}^-(u)$ , the only poles are simple, at  $\nu_0$  and  $w_1$ . The pole at  $w_1$  can be explained by figure 9 while, for  $\nu_0$ , we need figure 18. The second breather is emitted by the boundary, reducing it to the ground state, while a soliton is incident on the boundary at a rapidity  $w_1$ . For the ground state, this is neither a pole nor a zero, but the diagram contains a solitonic loop which can either be drawn to leave a soliton or an anti-soliton incident on the boundary. Adding the contributions of these two diagrams gives an additional zero.

For  $P_{|0;0,1\rangle}^+(u)$ , we have additional poles at all  $\nu$ , i.e. a simple pole at  $\nu_1$ , with  $\nu_0$  becoming a double pole. By lemma 1,  $\nu_1$  must correspond to the creation of a new bound state, namely  $|1;0,1,1\rangle$ , while, for  $\nu_0$ , figure 19 should be considered. Again, the second breather is created, the boundary is reduced to the ground state, and the breather is incident on the boundary at a rapidity of  $\frac{1}{2}(\nu_0 - w_1) = \xi/\lambda - \pi/2$  — a zero of the reflection factor.

### 5.6 Second level excited states — breather sector

For  $|0;0,1\rangle$ , we have the pole structure given in table 2.

	$-\frac{\xi}{\lambda} + \frac{3\pi}{2} + \frac{p\pi}{2\lambda}$	$-\frac{\xi}{\lambda} + \frac{\pi}{2} + \frac{p\pi}{2\lambda}$	$\frac{\xi}{\lambda} - \frac{\pi}{2} + \frac{p\pi}{2\lambda}$
$B_1$	-2	2	0, 2
$B_2$	-3	3	$1^2$

**Table 2: Breather pole structure for  $|0;0,1\rangle$ .**

The poles at  $-\frac{\xi}{\lambda} + \frac{3\pi}{2} + \frac{p\pi}{2\lambda}$  are due to figure 24, while the poles in the second column are due to figure 25. For all these, the boundary is reduced to  $|1;0\rangle$ . The pole at  $\frac{\xi}{\lambda} - \frac{\pi}{2} + \frac{(m-1)\pi}{2\lambda}$  for  $B_m$  ( $m = 2$ ) is due to figure 28, while for  $m = 1$  it is due to a breather version of figure 9. The pole at  $\frac{\xi}{\lambda} - \frac{\pi}{2} + \frac{2\pi}{2\lambda}$  for  $B_1$  is due to figure 23.

### 5.7 Third level excited states — soliton sector

The only third level excited state is  $|1; 0, 1, 1\rangle$ . For  $P_{[1;0,1,1]}^+$ , there are simple poles at  $w_1, \nu_0$  and  $\nu_1$ . Again, the pole at  $w_1$  comes from the crossed process figure 9. For  $\nu_1$ , figure 9 suffices while, for  $\nu_0$ , figure 20 is required, the boundary being reduced to  $|0; 0, 1\rangle$  while the first breather is incident on the boundary at  $\frac{\pi}{2} - \frac{\xi}{\lambda} + \frac{\pi}{\lambda}$ , another zero.

### 5.8 Third level excited states — breather sector

Here, the only possible boundary state is  $|1; 0, 1, 1\rangle$  and we find the poles given in table 3.

	$-\frac{\xi}{\lambda} + \frac{3\pi}{2} + \frac{p\pi}{2\lambda}$	$-\frac{\xi}{\lambda} + \frac{\pi}{2} + \frac{p\pi}{2\lambda}$	$\frac{\xi}{\lambda} - \frac{\pi}{2} + \frac{p\pi}{2\lambda}$	$\frac{\xi}{\lambda} + \frac{\pi}{2} + \frac{p\pi}{2\lambda}$
$B_1$	-2	$2^2, 4$	$0, 2$	—
$B_2$	-3	$1, 3^3$	$1^2$	-5

**Table 3: Breather pole structure for  $|1; 0, 1, 1\rangle$ .**

Comparing this with the structure given above for  $|1; 1\rangle$ , it can easily be seen that, whenever the two both have a pole at the same rapidity, essentially the same explanation can be used. For the remaining poles,  $-\frac{\xi}{\lambda} + \frac{3\pi}{2} + \frac{p\pi}{2\lambda}$  can be explained by figure 25, the boundary being reduced to  $|1; 0\rangle$ , while that at  $-\frac{\xi}{\lambda} + \frac{\pi}{2} + \frac{p\pi}{2\lambda}$  for  $B_2$  is due to figure 9, reducing the boundary to  $|1; 0\rangle$ , and that at  $\frac{\xi}{\lambda} - \frac{\pi}{2} + \frac{p\pi}{2\lambda}$  for  $B_1$  is due to an all-breather version of figure 23, again reducing the boundary to  $|1; 0\rangle$ .

### 5.9 Summary

The above has shown that, by introducing only the states which are required by lemmas 1 and 2, the complete pole structure can be explained. Below, we shall find that this is a general feature. In addition, the spectrum of states is broader than that introduced in [7] (containing, in addition to their states,  $|1; 0, 1, 1\rangle$ ). It should be noted that the mass of this extra state corresponds to  $m_{1,1}$  of [7], the mass of a boundary Bethe ansatz (1,1)-string whose apparent absence from the bootstrap spectrum was described in that paper as “confusing”. This does at least show that the Bethe ansatz results of [7] are not incompatible with the bootstrap. However, in more general cases it turns out that the bootstrap predicts yet further states, beyond those identified in the boundary Bethe ansatz calculations of [7], so a full reconciliation of the Bethe ansatz and bootstrap approaches remains an open problem.

## 6 The general case

From the above, we might be tempted to guess that the boundary state  $|c; n_1, n_2, n_3, \dots, n_m\rangle$  exists iff  $c$  is 0 or 1 and  $n_1, n_2, n_3, \dots$  are chosen such that  $\pi/2 > \nu_{n_1} > w_{n_2} > \nu_{n_3} > \dots > 0$ . This turns out to be correct, and will be proved in two stages. Firstly, we need to show that all these states must be present, before going on to show that, given this, all other poles can be explained without invoking further boundary states.

### 6.1 The minimal spectrum

The argument proceeds as follows: starting with the knowledge that the vacuum state  $|0\rangle$  and all appropriate states  $|1; n_1\rangle$  are in the spectrum, we use breather poles to construct all the other postulated states.

These poles are of the form  $\frac{1}{2}(w_N - \nu_n)$  for breather  $n + N$  incident on a charge 0 state (or  $\frac{1}{2}(\nu_n - w_N)$  for a charge 1 state). If  $\nu_n - w_N < \frac{\pi}{\lambda}$ , lemma 1 shows that they must correspond either to the formation of a new state, or the crossed process. From figure 11, this corresponds either to adding indices  $n$  and  $N$  if they are absent or — if they are already present — removing them. (Note that any other option would give rise to a state with a mass outside the scheme given by (36), and therefore outside our postulated spectrum.) The condition  $\nu_n - w_N < \frac{\pi}{\lambda}$  is always satisfied if  $\nu_n > w_N$  and  $\nu_n$  and  $w_N$  are as close together as possible, i.e. if  $|0; n, N\rangle$  exists, but  $|0; n, N - 1\rangle$  does not.



The only subtlety in this argument arises when considering the topmost breather. If  $n + N = n_{max}$ , lemma 1 on its own is not strong enough to require the presence of the state we need, and we must invoke the stronger version introduced at the end of section 3. This makes use the idea that there must be a corresponding two-stage solitonic route to the same state, i.e. a soliton with rapidity  $\nu_n$  followed by an anti-soliton with rapidity  $w_N$ . Considering these two processes instead, the stronger lemma shows that both form bound states, as  $\nu_n$  and  $w_N$  must be the lowest poles of their type — and so have rapidity less than  $\frac{\pi}{\lambda}$  — for  $n + N$  to equal  $n_{max}$ . This shows that the state exists, and hence that the breather pole is due to its formation.

Since the arguments for the two sectors are analogous, let us focus on the charge 0 sector here. The challenge is to create any state  $|0; \underline{x}\rangle$  — for some set of indices  $\underline{x} = (n_1, n_2, \dots, n_{2k})$  — from the ground state using just these poles. As a first step, consider creating  $|0; n_1, n_2\rangle$ . If  $\nu_{n_1}$  and  $w_{n_2}$  are as close together as possible, we simply make use of the pole at  $\frac{1}{2}(w_{n_2} - \nu_{n_1})$ . Otherwise, introduce the set  $m_1, m_2, \dots, m_t$  such that  $\nu_{n_1} > w_{m_1} > \nu_{m_2} > w_{m_3} > \dots > \nu_{m_t} > w_{n_2}$ , with each successive rapidity as close to the previous one as possible. Now, we can successively create  $|0; \underline{x}, n_1, m_1\rangle$ , then  $|0; \underline{x}, n_1, m_1, m_2, m_3\rangle$  and so on, up to  $|0; \underline{x}, n_1, m_1, m_2, m_3, \dots, m_t, n_2\rangle$ .

By now invoking the crossed process, a suitable breather can be used to removed the indices  $m_1, m_2$ , followed by  $m_3, m_4$  and so on, until all the  $m$  indices have been removed to leave  $|0; \underline{x}, n_1, n_2\rangle$ .

Repeating this procedure allows  $|0; n_1, n_2, n_3, n_4\rangle$  to be created, and hence  $|0; \underline{x}\rangle$ . Note that this allows any state in our allowed spectrum to be created, but no others, as the condition  $\nu_{n_1} > w_{n_2} > \dots$  is imposed by the existence of the necessary breather poles. Charge 1 states can be created analogously by starting from a suitable state  $|1; n_1\rangle$ .

One remaining point is to check that all the necessary breather poles do indeed exist. However, starting from (38), they occur in the  $R_{(c)}^n(u)$  factor, and it is straightforward to check that they are never modified by the other  $a$  factors.

## 6.2 Reflection factors for the minimal spectrum

The boundary state can be changed by the solitonic processes given in table 4.

Initial state	Particle	Rapidity	Final state
$ 0; n_1, \dots, n_{2k}\rangle$	Soliton	$\nu_n$	$ 1; n_1, \dots, n_{2k}, n\rangle$
$ 1; n_1, \dots, n_{2k-1}\rangle$	Anti – soliton	$w_N$	$ 0; n_1, \dots, n_{2k-1}, N\rangle$

**Table 4: Solitonic processes which change the boundary state.**

The breather sector is more complex, as indices can be added or removed from any point in the list, and not just at the end, as for solitons. In addition, processes exist which simply adjust the value of one of the indices, rather than increasing the number of indices. For breather  $m$ , these are given in table 5. This should be read as implying that any index can have its value raised, and that a pair of indices can be

Initial state	Rapidity	Final state
$ 0/1; n_1, \dots, n_{2x}, n_{2x+1}, \dots\rangle$	$\frac{1}{2}(\nu_n - w_N), n + N = m$	$ 0/1; n_1, \dots, n_{2x}, n, N, n_{2x+1}, \dots\rangle$
$ 0/1; n_1, \dots, n_{2x-1}, n_{2x}, \dots\rangle$	$\frac{1}{2}(w_N - \nu_n), n + N = m$	$ 0/1; n_1, \dots, n_{2x-1}, N, n, n_{2x}, \dots\rangle$
$ 0/1; n_1, \dots, n_{2x}, \dots\rangle$	$\frac{1}{2}(\nu_{-n_{2x}} - w_{n_{2x}+m})$	$ 0/1; n_1, \dots, n_{2x} + m, \dots\rangle$
$ 0/1; n_1, \dots, n_{2x-1}, \dots\rangle$	$\frac{1}{2}(w_{-n_{2x-1}} - w_{n_{2x-1}+m})$	$ 0/1; n_1, \dots, n_{2x-1} + m, \dots\rangle$

**Table 5: Breather processes which change the boundary state.**

inserted at any point in the list, including before the first index and after the last (providing the resultant state is allowed). Both these tables have been derived on the basis that, whenever assuming that a pole corresponds to a bound state leads to a state with the same mass and topological charge as one in our minimal spectrum, the assumption is taken to be correct. As with our earlier assumption (that, if a pole has another possible explanation, it is not taken as forming a bound state), this is intuitively reasonable but



not necessarily rigorous. It does, however, lead to consistent results, and there is no conflict between the two assumptions: we have been unable to find any alternative explanation for any of the poles listed above.

It is vital for what follows that, for all the above processes, there is very little dependence on the existing boundary state. For the solitons, the topological charge of the state and the value of the last index in the list are all that matter. Any two states which have the same topological charge and last index can undergo processes at the same rapidities to add an index. Similarly, for the breathers, provided either the relevant two indices can be added at some point in the list to create an allowed state, or that the index to be adjusted is present in the list, the other characteristics of the state are irrelevant.

### 6.3 Solitonic pole structure

This turns out to be relatively straightforward. All poles are either of the form  $\nu_n$  or  $w_N$ . Looking at a charge 0 state with  $2k$  indices, and labelling this as  $\underline{x} = (n_1, n_2, \dots, n_{2k})$ , we find the results shown in table 6 for  $P_{|0;\underline{x}\rangle}^-(u)$ . These poles come from the  $a$  factors so, for  $P^+$ , there is an additional pole at all  $\nu$ .

Pole	Order	Pole
$w_1 \dots w_{n_2-1}$	$2k$	$\nu_1 \dots \nu_{n_1-1}$
$w_{n_2}$	$2k-1$	$\nu_{n_1}$
$w_{n_2+1} \dots w_{n_4-1}$	$2k-2$	$\nu_{n_1+1} \dots \nu_{n_3-1}$
$w_{n_4}$	$2k-3$	$\nu_{n_3}$
$\vdots$	$\vdots$	$\vdots$
$w_{n_{2k-2}+1} \dots w_{n_{2k}-1}$	$2$	$\nu_{n_{2k-3}+1} \dots \nu_{n_{2k-1}-1}$
$w_{n_{2k}}$	$1$	$\nu_{n_{2k-1}}$

**Table 6: Pole structure for  $P_{|0;\underline{x}\rangle}^-(\mathbf{u})$ .** An entry of, for example,  $w_1 \dots w_{n_2-1}$  indicates that there is a pole of order  $2k$  at  $w_1, w_2, w_3, \dots, w_{n_2-1}$ .

For the charge 1 states, the picture is very similar, and, considering first the  $a$  factors, we find the pattern given in table 7 for a state with  $2k-1$  indices. For  $P^-$  there are additional poles at all  $w$ . (For the charge 0 case, there are poles at  $w_x$  for  $x \leq 0$ , but none of these are in the physical strip.)

Pole	Order	Pole
—	$1$	$\nu_{-1}, \nu_{-2} \dots$
—	$k$	$\nu_0$
—	$2k$	$\nu_1 \dots \nu_{n_1-1}$
—	$2k-1$	$\nu_{n_1}$
$w_1 \dots w_{n_2-1}$	$2k-2$	$\nu_{n_1+1} \dots \nu_{n_3-1}$
$w_{n_2}$	$2k-3$	$\nu_{n_3}$
$\vdots$	$\vdots$	$\vdots$
$w_{n_{2k-4}+1} \dots w_{n_{2k-2}-1}$	$2$	$\nu_{n_{2k-3}+1} \dots \nu_{n_{2k-1}-1}$
$w_{n_{2k-2}}$	$1$	$\nu_{n_{2k-1}}$

**Table 7: Pole structure for  $P_{|1;\underline{x}\rangle}^+(\mathbf{u})$ .**

An important point to note is that, comparing a general level  $2k$  state  $|0; n_1, n_2, \dots, n_{2k-1}, n_{2k}\rangle$  with the level 2 state  $|0; n_{2k-1}, n_{2k}\rangle$ , we find no additional poles, though the order of some poles has increased. In the example above, all level 2 states were explained by diagrams where the boundary was reduced either to the vacuum by emission of a breather, or to a first level excited state by emission of an anti-soliton. The same processes turn out to be present for any level  $2k$  state to be reduced to a level  $2k-1$  or  $2k-2$  state. Thus, we might imagine explaining the poles in the level  $2k$  reflection factor via similar processes to the ones which explained them in the level 2 factor. At times, however — as we shall see — parts of these processes will need to be replaced by more complex subdiagrams to allow for the fact that the boundary

is in a higher excited state, explaining the differences in the orders of the poles. Considering the level 2 processes so far introduced as “building blocks”, this can be considered as an iterative process: level 4 states can be explained by replacing parts of level 2 processes with building blocks, while level 6 states can be explained by similarly replacing parts of level 4 processes with building blocks, and so on. A generic process of the type we will examine can therefore be viewed as a cascade of building blocks, each appearing as a subdiagram of the one before it.

A similar argument applies to level  $2k + 1$  states and level 3 states, drawing the same diagrams with all rapidities transformed via  $\xi \rightarrow \pi(\lambda + 1) - \xi$ . We will concentrate on the charge 0 sector below, and consider a generic level  $2k$  state.

For poles of the form  $\nu_n$ , consider figure 29. The boundary decays to the state  $|0; n_1, n_2, \dots, n_{2k-2}\rangle$  by emission of breather  $n_{2k} + n_{2k-1}$  at a rapidity of  $\frac{1}{2}(\nu_{n_{2k-1}} - w_{n_{2k}})$ . This then decays into breather  $n_{2k-1} - n$  heading towards the boundary at a rapidity of  $\frac{1}{2}(w_{-n_{2k-1}} - \nu_n)$  and breather  $n_{2k} + n$  heading away from the boundary at a rapidity of  $\nu_n - \left(\frac{\pi}{2} - \frac{(n_{2k} + n)\pi}{2\lambda}\right)$ . This then decays to give the outgoing particle and one heading towards the boundary at a rapidity of  $w_{n_{2k}}$ . For  $n < n_{2k-1}$ , it is straightforward to check that all these rapidities are within suitable bounds.

This diagram is naïvely third order. However, breather  $n_{2k-1} - n$ , which is drawn as simply reflecting off the boundary, in fact has a pole, meaning that the diagram should be treated as schematic and the appropriate diagram from the next section inserted instead. In addition, as noted in the discussion of the example, the soliton loop contributes a zero for an incoming anti-soliton through the Coleman-Thun mechanism. When this is taken into account, we obtain the correct result.

For  $\nu_{n_{2k-1}}$ , the slightly simpler figure 18 suffices. The remaining  $\nu$  poles are only present in the soliton reflection factor, and can be explained by figure 19, with the boundary decaying by emitting an anti-soliton at  $w_{n_{2k}}$ , which then interacts with the incoming soliton to give breather  $n + n_{2k}$ , heading towards the boundary at a rapidity of  $\frac{1}{2}(\nu_n - w_{n_{2k}})$ . Looking ahead again, the interaction of this breather with the boundary contributes the required zero. For  $\nu_n < w_{n_{2k}}$ , this diagram fails, the breather being created heading away from the boundary; this is the point when the pole is to be considered as creating the bound state  $|1; n_1, \dots, n_{2k}, n\rangle$ .

For the  $w_N$  poles, the story is very similar, this time being based on figure 20 (requiring a suitable pole/zero for  $B_{N-n_{2k}}$  on state  $|1; n_1, \dots, n_{2k-1}\rangle$  at  $\frac{\xi}{\lambda} - \frac{\pi}{2} + \frac{\pi(N+n_{2k}-1)}{2\lambda}$ ) for  $N < n_{2k}$  and figure 9 for  $n_{2k}$ . As noted above, all charge 1 state poles can be explained by the same mechanisms, with the rapidities transformed according to  $\xi \rightarrow \pi(\lambda + 1) - \xi$ .

#### 6.4 Breather pole structure

This is considerably more complicated. However, with a bit of work it turns out that, for breather  $n$  on the state  $|0; n_1, n_2, \dots, n_{2k}\rangle$ , the pole structure is as given in table 8.

Pole	Range	Pole/zero order
$\frac{\xi}{\lambda} - \frac{\pi}{2} + \frac{\pi(n+2x-1)}{2\lambda}$	$n_{2q} < x < n_{2q+2}, n_{2q'} < n + x < n_{2q'+2}$	$2(q' - q) + y$
$-\frac{\xi}{\lambda} + \frac{\pi}{2} + \frac{\pi(n+2x+1)}{2\lambda}$	$x < 0, n_{2q-1} <  x  < n_{2q+1}, n_{2q'} < n -  x  < n_{2q'+2}$	$2(q' - q) + y + i$
	$n_{2q-1} < x < n_{2q+1}, n_{2q'-1} < n + x < n_{2q'+1}$	$2(q' - q) + y$
	$x < 0, n_{2q} <  x  < n_{2q+2}, n_{2q'-1} < n -  x  < n_{2q'+1}$	$2(q' - q) - i + y$
	$x < -n, n_{2q} <  x  < n_{2q+2}, n_{2q'} <  x  - n < n_{2q'+2}$	$2(q' - q)$
$\frac{\xi}{\lambda} + \frac{\pi}{2} + \frac{\pi(n+2x-1)}{2\lambda}$	As $\frac{\xi}{\lambda} - \frac{\pi}{2} + \frac{\pi(n+2x+1)}{2\lambda}$ with poles $\leftrightarrow$ zeroes	
$-\frac{\xi}{\lambda} + \frac{3\pi}{2} + \frac{\pi(n+2x+1)}{2\lambda}$	As $-\frac{\xi}{\lambda} + \frac{\pi}{2} + \frac{\pi(n+2x-1)}{2\lambda}$ with poles $\leftrightarrow$ zeroes	

**Table 8: Breather pole structure for a generic charge 0 state.** The variable  $x$  takes integer and half-integer values within the allowed ranges. An entry in the third column represents a pole of that order if it is positive, and a zero of appropriate order if it is negative. (Thus an entry of +1 is a first-order pole, and an entry of -1 is a first-order zero.) Also, for convenience,  $y$  is 1 if  $x$  (or  $|x|$ ) attains the lower limit, -1 if  $n + x$  (or  $n - |x|$ ) attains the lower limit, and zero otherwise, while  $i$  is 1 if  $x$  is integer, and 0 otherwise.

In explaining all this, we can begin with the diagrams found previously. For the first line, consider an all-breather version of figure 21, where the breather decay is chosen to produce breather  $n + x - n_{2q'}$  on the left, which then binds to the boundary to raise index  $n_{2q'}$  to  $n + x$ . In some cases, this is not possible, the appropriate state not being in the spectrum, but, then, we can consider an all-breather version of figure 26, where the boundary decays so as to remove the indices  $n_{2q'}$  and  $n_{2q'+1}$ , with the same initial breather decay, and the additional breather reflecting from the boundary contributes a zero. This diagram becomes possible just as the other fails. In either case, the other breather from the initial decay (which is drawn as simply reflecting from the boundary), is breather  $y = n_{2q'} - x$  at rapidity  $\frac{\xi}{\lambda} - \frac{\pi}{2} + \frac{\pi(y+2x-1)}{2\lambda}$ . This has a pole of order 2 less than the initial breather. If this order is less than or equal to zero, the diagram stands as drawn while, otherwise, the simple reflection from the boundary should be replaced by a repeat of this argument, iterating until the result is less than or equal to zero. For the next line, precisely the same argument can be used.

The next three lines can be explained by a similar argument, based on either increasing the value of index  $n_{2q'-1}$  or removing indices  $n_{2q'-1}$  and  $n_{2q'}$ .

For  $\frac{\xi}{\lambda} + \frac{\pi}{2} + \frac{\pi(n+2x-1)}{2\lambda}$ , we invoke a similar process. This time, however, the outer legs have rapidity  $\nu_{-(n+x)}$  (where  $-(n+x)$  is actually a positive number if the initial pole is to be in the physical strip), and so we need to substitute in the explanation of soliton poles of this form from before, leading, in simple cases, to figure 25.

Finally, for  $\frac{3\pi}{2} - \frac{\xi}{\lambda} + \frac{\pi(n+2x+1)}{2\lambda}$ , we begin with figure 24. This time, the reflection factor for the central soliton always provides a zero, while the outer soliton has rapidity  $w_{n+x}$ . If  $n + x = n_{2k}$ , the diagram is as drawn while, otherwise, we need to replace the two outer anti-soliton legs with the explanation of the appropriate pole in the anti-soliton factor. The first iteration of this is shown in figure 26.

## 7 Conclusions

We now summarise our results. We have found that the spectrum of boundary bound states of the sine-Gordon model with Dirichlet boundary conditions can be characterised in terms of two “sectors”, having topological charges  $\frac{\beta\varphi_0}{2\pi}$  and  $1 - \frac{\beta\varphi_0}{2\pi}$  (which we labelled as “0” and “1” respectively). A boundary state can be described in an index notation as  $|c; n_1, n_2, \dots, n_k\rangle$  for topological charge  $c$ , with  $c = 0$  for  $k$  even and  $c = 1$  for  $k$  odd. Such a state can be created by a succession of alternating solitons and anti-solitons, beginning with a soliton. The necessary soliton rapidities are of the form,

$$\nu_n = \frac{\xi}{\lambda} - \frac{\pi(2n+1)}{2\lambda}, \quad (46)$$

while those for the anti-solitons are

$$w_m = \pi - \frac{\xi}{\lambda} - \frac{\pi(2m-1)}{2\lambda}. \quad (47)$$

These are interchanged by the transform  $\xi \rightarrow \pi(\lambda+1) - \xi$ . Any such state can be formed, provided the rapidities involved are monotonically decreasing, i.e.  $\nu_{n_1} > w_{n_2} > \nu_{n_3} > \dots$ , and its mass is given by

$$\begin{aligned} m_{n_1, n_2, \dots} &= m_s \sin^2 \left( \frac{\xi - \frac{\pi}{2}}{2\lambda} \right) + \sum_{i \text{ odd}} m_s \cos(\nu_{n_i}) + \sum_{j \text{ even}} m_s \cos(w_{n_j}) \\ &= m_s \sin^2 \left( \frac{\xi - \frac{\pi}{2}}{2\lambda} \right) + \sum_{i \text{ odd}} m_s \cos \left( \frac{\xi}{\lambda} - \frac{(2n_i+1)\pi}{2\lambda} \right) - \sum_{j \text{ even}} m_s \cos \left( \frac{\xi}{\lambda} + \frac{(2n_j-1)\pi}{2\lambda} \right). \end{aligned} \quad (48)$$

This spectrum is considerably larger than that suggested in [7], though all the states introduced are required to satisfy our lemmas. It is worth pointing out that a second part of the analysis of [7] involved an examination of the (boundary) Bethe ansatz for a lattice regularisation of the model. Some of the masses which emerged in the course of that study – those of the  $(n, N)$ -strings – were outwith the spectrum proposed in [7], but are now included as the masses of the states  $|1; 0, n, N\rangle$ . It remains to be seen, however, whether the other masses in our spectrum can be recovered in the Bethe ansatz approach.

The number of states present in the spectrum clearly depends on the boundary parameters, as illustrated in figure 16. It is convenient to express these in terms of Fibonacci numbers,  $F(x)$ , where

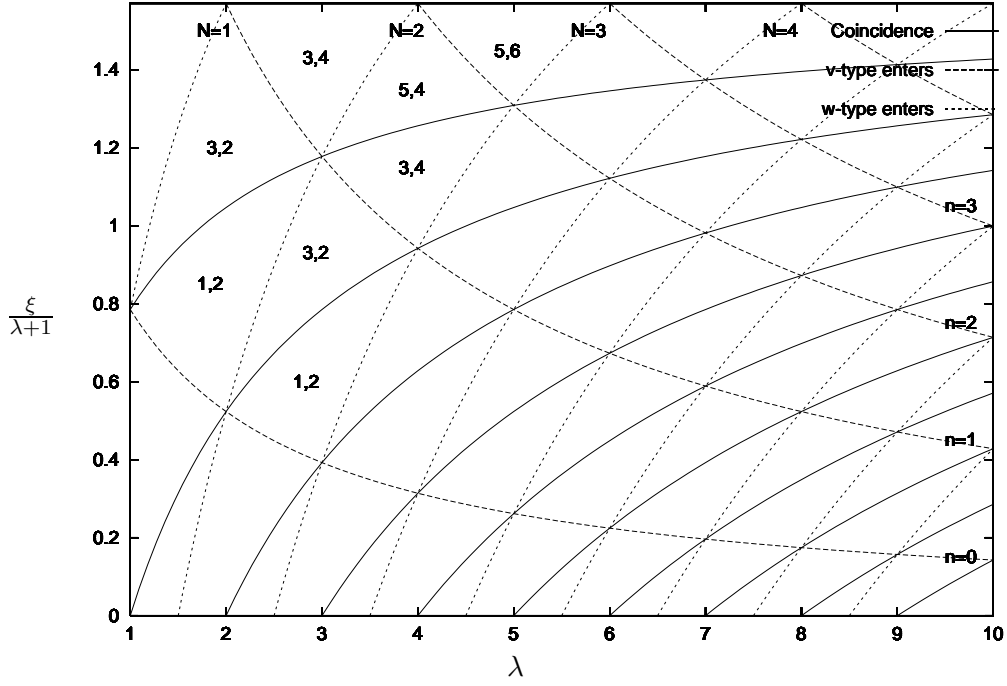


**Figure 16: Boundary bound state spectrum size.** The number of states present increases as  $\nu$ -type and  $w$ -type poles enter the physical strip, but changes also occur as the two sets of poles pass through coincidence: moving in the direction of increasing  $\lambda$ , the topmost relevant  $w$ -type pole passes  $\nu_0$  and ceases to be relevant, reducing the spectrum. (Notation  $x, y$  implies  $F(x)$  charge 0 states and  $F(y)$  charge 1 states.)

$F(x) = 1, 1, 2, 3, 5, \dots$  for  $x = 0, 1, 2, \dots$ . If there are  $n$   $\nu$ -type poles, and  $m$  relevant<sup>4</sup>  $w$ -type poles, there are, in general,  $F(2n)$  charge 1 states and  $F(2m + 1)$  charge 0 states. Explicitly, these are given by

$$n = \left\lfloor \frac{\xi}{\pi} - \frac{1}{2} \right\rfloor + 1 \quad \text{and} \quad m = \left\lfloor \frac{\lambda}{2} - \frac{\xi}{\pi} + \frac{1}{2} \right\rfloor - \left\lfloor \lambda - \frac{\xi}{\pi} + \frac{1}{2} \right\rfloor, \quad (49)$$

where the square brackets denote the integer part of the number. This changes when the two sets of poles coincide, in which case there are  $2^{n-1}$  states in each sector.

Finally we note that the general method used to derive the spectrum, via the simple geometrical argument leading to the two lemmas given in section 3, which can be applied equally well to any two-dimensional model. Using this to deduce the existence of as many states as possible led — in our case — to the full spectrum. In other cases, we may not be so fortunate, but, using it as a starting point, it should make the derivation of the full spectrum a finite (though possibly lengthy) task.

**Acknowledgements** — We are grateful to Aldo Delfino, Subir Ghoshal, Brett Gibson and Matthias Pillin for help and interesting discussions. We would especially like to thank Gustav Delius for his comments on a first draft of this paper. PM and PED thank the EPSRC for a Research Studentship and an Advanced Fellowship respectively, and PED thanks SPhT Saclay and the Departamento de Física de Partículas, USC (Santiago de Compostela), for hospitality. The work was supported in part by a TMR grant of the European Commission, reference ERBFMRXCT960012. Finally, we are also grateful to Zoli Bajnok and Gabor Takács for pointing out a number of typos in version one of this paper.

## A Infinite products of gamma functions

The products which arise in the course of this work are of the form

$$P(u) = \prod_{l=1}^{\infty} \left[ \frac{\Gamma(kl + a - xu)\Gamma(kl + b - xu)}{\Gamma(kl + c - xu)\Gamma(kl + d - xu)} / (u \rightarrow -u) \right], \quad (A.1)$$

<sup>4</sup>A  $w$ -type pole with a rapidity greater than  $\nu_0$  can never be involved in forming a bound state, and so is not “relevant” here.

Rather than examine this product directly, we take logs and use the standard formula

$$\ln \Gamma(z) = z \ln(z) - z - \frac{1}{2} \ln(z) + \ln(\sqrt{2}) + \frac{1}{12z} + O(z^{-3}) \quad (\text{A.2})$$

Assuming that the sum over  $l$  and the expansion in  $z$  can be exchanged, potential divergences arise from terms of the form  $\sum_{l=1}^{\infty} \frac{a}{l^n}$  with  $a \neq 0$  and  $n < 2$ . To begin with, we will consider the terms arising from the block of four terms explicitly shown.

Firstly, there is a contribution of  $\sum_{l=1}^{\infty} a + b - c - d$  from the  $z$  terms, which can be set to zero by demanding  $a + b = c + d$ . For the  $1/12z$  terms, the overall contribution from the four terms is

$$\sum_{l=1}^{\infty} \frac{1}{12} \left( \frac{a - c}{(kl + a - xu)(kl + c - xu)} + \frac{b - d}{(kl + b - xu)(kl + d - xu)} \right) \quad (\text{A.3})$$

which can be seen, for  $a + b = c + d$ , to be of the form  $1/l^2$  and hence convergent.

A similar argument applies to the  $-\frac{1}{2} \ln(z)$  terms, showing they also provide a convergent contribution. This breaks down when considering the  $z \ln(z)$  terms, however, and their contribution formally reduces to

$$\sum_{l=1}^{\infty} \left( \frac{cd - ab}{kl} + O(l^{-2}) \right), \quad (\text{A.4})$$

which is divergent unless  $a = c$  or  $b = c$ , both of which are trivial cases. However, repeating this argument on the other block (with  $u \rightarrow -u$ ) can be seen to yield the same result, allowing the two divergent terms to cancel, and leaving a product which is convergent overall.

For comparison with other results, it is useful to write  $P(u)$  in other ways. Firstly, it can be written in terms of Barnes' diperiodic sine functions using the expansion as given in [11]:

$$\begin{aligned} S_2(x|\omega_1, \omega_2) &= \exp \left[ \frac{(\omega_1 + \omega_2 - 2x) \left( \gamma + \log(2\pi) + 2 \log \left( \frac{\omega_1}{\omega_2} \right) \right)}{2\omega_1} \right] \frac{\Gamma \left( \frac{\omega_1 + \omega_2 - x}{\omega_1} \right)}{\Gamma \left( \frac{x}{\omega_1} \right)} \times \\ &\quad \prod_{n=1}^{\infty} \left[ \frac{\Gamma \left( \frac{\omega_1 + \omega_2 - x + n\omega_2}{\omega_1} \right)}{\Gamma \left( \frac{x + n\omega_2}{\omega_1} \right)} e^{-\frac{\omega_1 + \omega_2 - 2x}{2n\omega_1}} \left( \frac{n\omega_1}{\omega_2} \right)^{-\frac{\omega_1 + \omega_2 - 2x}{\omega_1}} \right], \end{aligned} \quad (\text{A.5})$$

where  $\gamma$  denotes the Euler constant. For blocks of the form we are interested in, this simplifies to

$$\begin{aligned} \frac{S_2(x_1|\omega_1, \omega_2) S_2(x_2|\omega_1, \omega_2)}{S_2(x_3|\omega_1, \omega_2) S_2(x_4|\omega_1, \omega_2)} &= \\ \prod_{n=1}^{\infty} \left[ \left\{ \frac{\Gamma \left( \frac{n\omega_2}{\omega_1} + \frac{\omega_1 - \omega_2}{2\omega_1} - \frac{x'_1}{2\omega_1} \right) \Gamma \left( \frac{n\omega_2}{\omega_1} + \frac{\omega_1 - \omega_2}{2\omega_1} - \frac{x'_2}{2\omega_1} \right)}{\Gamma \left( \frac{n\omega_2}{\omega_1} + \frac{\omega_1 - \omega_2}{2\omega_1} - \frac{x'_3}{2\omega_1} \right) \Gamma \left( \frac{n\omega_2}{\omega_1} + \frac{\omega_1 - \omega_2}{2\omega_1} - \frac{x'_4}{2\omega_1} \right)} \right\} / (x'_m \rightarrow -x'_m) \right], \end{aligned} \quad (\text{A.6})$$

(where  $x'_m = x_m - \omega_1 - \omega_2$ ) provided  $x_1 + x_2 = x_3 + x_4$ . Comparing with (A.1) we have

$$P(u) = \frac{S_2(\omega_1(1 - a + xu)|\omega_1, \omega_1 k) S_2(\omega_1(1 - b + xu)|\omega_1, \omega_1 k)}{S_2(\omega_1(1 - c + xu)|\omega_1, \omega_1 k) S_2(\omega_1(1 - d + xu)|\omega_1, \omega_1 k)}, \quad (\text{A.7})$$

where  $w_1$  is arbitrary. In section 2 we took  $\omega_1 = x^{-1}$  for simplicity. The identity

$$S_2(\omega_1 + \omega_2 - x|\omega_1, \omega_2) = \frac{1}{S_2(x|\omega_1, \omega_2)} \quad (\text{A.8})$$

was also used.

These products can also be written in an integral form, through

$$\log \Gamma(\zeta) = \int_0^{\infty} \frac{dx}{x} e^{-x} \left[ \zeta - 1 + \frac{e^{-(\zeta-1)x} - 1}{1 - e^{-x}} \right], \quad \text{Re } \zeta > 0. \quad (\text{A.9})$$

Since, for the expressions we consider, not all the  $\Gamma$ -functions have arguments with positive real part, it is not possible to give a general formula for  $P$  solely in these terms. Instead, we give expressions for the reflection factors. To simplify matters, define

$$I^1(u) = \frac{2\lambda}{\pi} \int_{-\infty}^{+\infty} dx \cosh\left(\frac{2\lambda ux}{\pi}\right) \left[ \frac{\sinh\left(\lambda - \frac{2\xi}{\pi}\right)x}{2 \sinh x \cosh \lambda x} \right] \quad (\text{A.10})$$

$$I^2(u) = \frac{2\lambda}{\pi} \int_{-\infty}^{+\infty} dx \cosh\left(\frac{2\lambda ux}{\pi}\right) \left[ \frac{\sinh\left(\frac{2\xi}{\pi} - 2n_* - 2\right)x}{\sinh x} \right] \quad (\text{A.11})$$

$$I_n^3(u) = -\frac{2\lambda}{\pi} \int_{-\infty}^{+\infty} dx \cosh\left(\frac{2\lambda ux}{\pi}\right) \left[ \frac{2 \cosh x \sinh\left(\lambda + 1 + 2n - \frac{2\xi}{\pi}\right)x}{2 \sinh x \cosh \lambda x} \right] \quad (\text{A.12})$$

$$I_n^4(u) = -\frac{2\lambda}{\pi} \int_{-\infty}^{+\infty} dx \cosh\left(\frac{2\lambda ux}{\pi}\right) \left[ \frac{2 \cosh x \sinh\left(\frac{2\xi}{\pi} + 2n - \lambda - 1\right)x}{2 \sinh x \cosh \lambda x} \right] \quad (\text{A.13})$$

(where  $I_n^3(u)$  and  $I_n^4(u)$  are related to each other through  $\xi \rightarrow \pi(\lambda + 1) - \xi$ ). The constant  $n_*$  is the number of  $\nu$ -type poles in the physical strip, which we recall can be written as

$$n_* = \left\lfloor \frac{\xi}{\pi} - \frac{1}{2} \right\rfloor. \quad (\text{A.14})$$

The reflection factors can then be written as

$$-\frac{d}{du} \log \left[ \frac{P_{[c;\underline{x}]}^+(u)}{R_0(u)} \right] = I^1(u) + cI^2(u) + \sum_{i \text{ odd}} I_{n_i}^3(u) + \sum_{j \text{ even}} I_{n_j}^4(u) \quad (\text{A.15})$$

$$-\frac{d}{du} \log \left[ \frac{P_{[c;\underline{x}]}^-(u)}{R_0(u)} \right] = I^1(u) - (1-c)I^2(u) + \sum_{i \text{ odd}} I_{n_i}^3(u) + \sum_{j \text{ even}} I_{n_j}^4(u), \quad (\text{A.16})$$

for topological charge  $c$  and  $\underline{x} = (n_1, n_2, \dots, n_{2k+c})$ . These factors were given in [7] for the first two levels of excited states (the extent of the spectrum they found); the above is simply a generalisation of this to the whole spectrum.

## B On-shell diagrams

In this appendix we collect together some of the on-shell diagrams used in the main body of the paper. All boundaries are initially in the state  $|n_1, n_2, \dots, n_{2k}\rangle$ , where  $k$  can be any integer, and we have suppressed the topological charge index (which is zero). Analogous processes for charge 1 states can be found by applying the transformation  $\xi \rightarrow \pi(\lambda + 1) - \xi$  to all rapidities shown.

In addition, where the boundary is shown decaying through emission of a breather, only the process where this removes the last two indices is given. Similar processes always exist to remove any other adjacent pair of indices, or to simply modify an index; see section 6.2 for the appropriate breather boundary vertices.

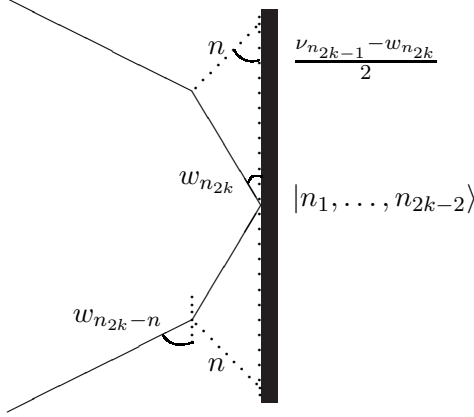


Figure 17: Soliton, breather boundary decay

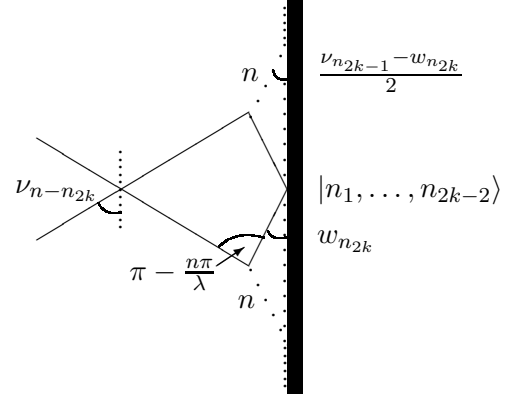


Figure 18: Incoming soliton crossed

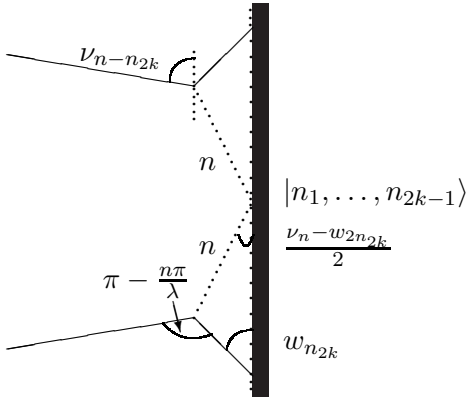


Figure 19: Soliton, soliton boundary decay

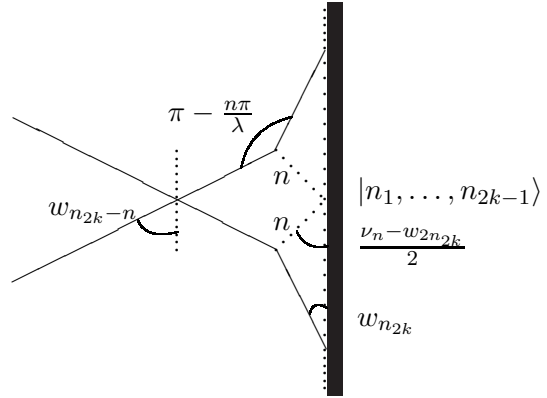


Figure 20: Incoming soliton crossed

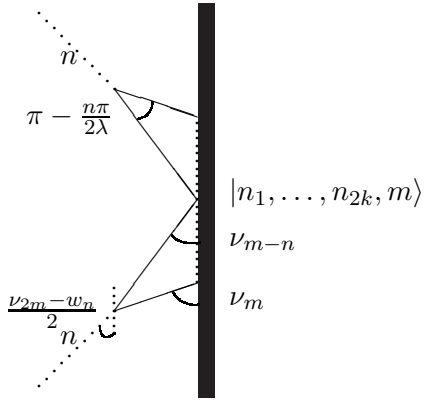


Figure 21: Breather, soliton bound state

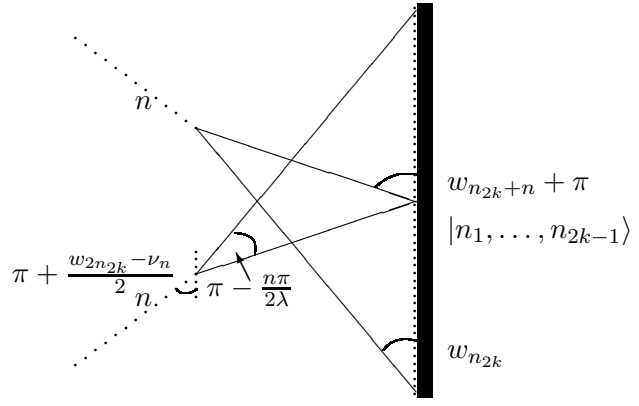


Figure 22: Outgoing soliton crossed

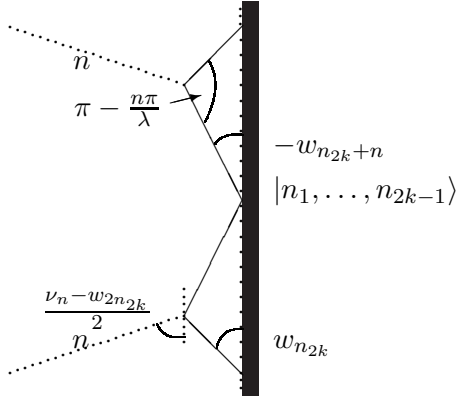


Figure 23: Breather, soliton boundary decay

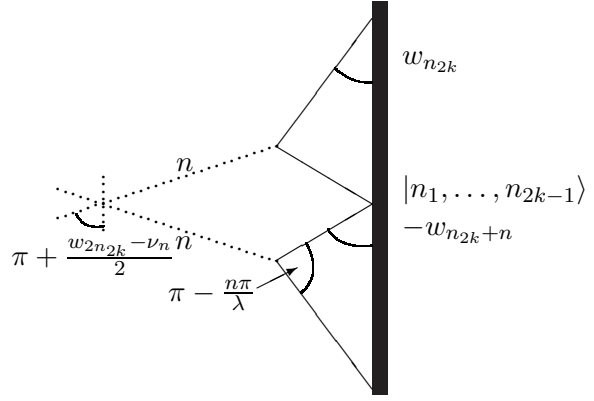


Figure 24: Incoming breather crossed

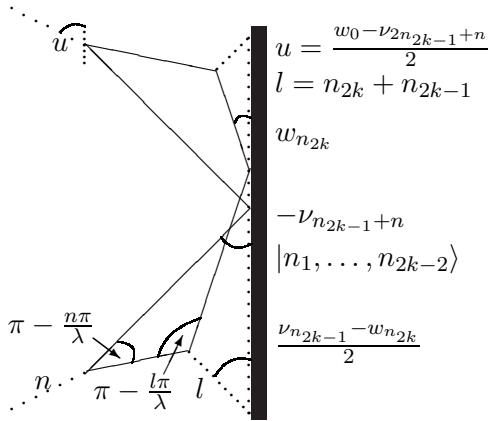


Figure 25: As 21, outer legs replaced by 17

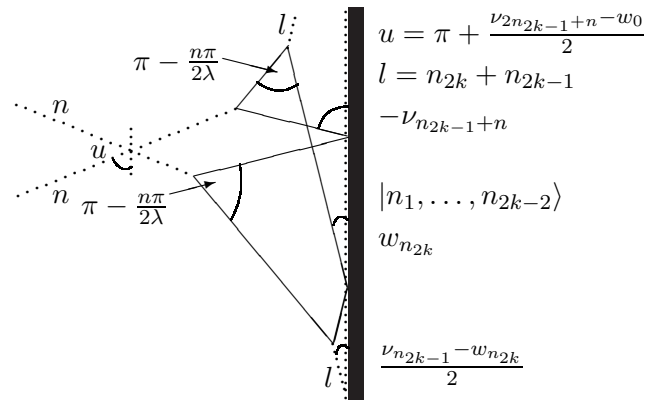


Figure 26: As 24, outer legs replaced by 18



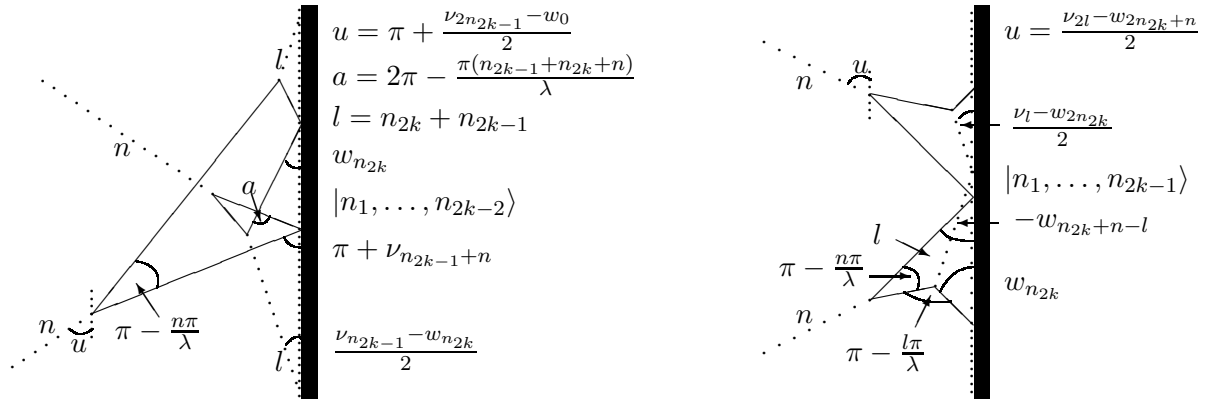


Figure 27: As 22, outer legs replaced by 18      Figure 28: As 21, outer legs replaced by 19

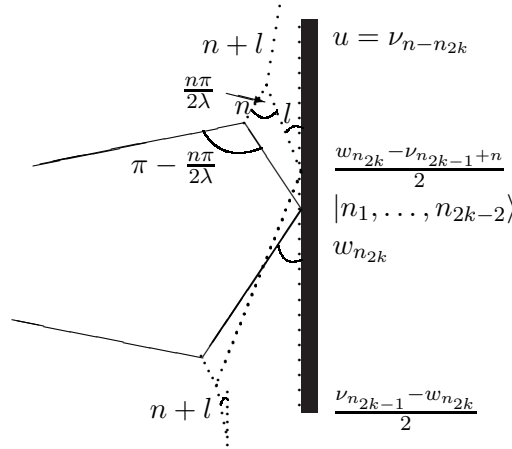


Figure 29: As 18, outer legs replaced by all-breather version

## References

- [1] S. Ghoshal and A. Zamolodchikov, *Boundary S matrix and boundary state in two-dimensional integrable quantum field theory*, Int. J. Mod. Phys. **A9** (1994) 3841–3885, preprint [hep-th/9306002](#)
- [2] C. Kane and M. Fisher, *Transmission through barriers and resonant tunneling in an interacting one-dimensional electron gas*, Phys. Rev. **B46** (1992) 15233–15262
- [3] X.G. Wen, *Chiral Luttinger liquid and the edge excitations in the fractional quantum Hall states*, Phys. Rev. **B41** (1990) 12838–12844
- [4] P. Fendley, A.W.W. Ludwig and H. Saleur, *Exact Conductance through Point Contacts in the  $\nu = 1/3$  Fractional Quantum Hall Effect*, Phys. Rev. Lett. **74** (1995) 3005–3008, preprint [cond-mat/9408068](#)
- [5] H. Saleur, *Lectures on non perturbative field theory and quantum impurity problems*, in the proceedings of the 1998 Les Houches Summer School, preprint [cond-mat/9812110](#)  
H. Saleur, *Lectures on non perturbative field theory and quantum impurity problems. Part II*, preprint [cond-mat/0007309](#)
- [6] S. Ghoshal, *Bound State Boundary S-Matrix of the sine-Gordon Model*, Int. J. Mod. Phys. **A9** (1994) 4801–4810, preprint [hep-th/9310188](#)

- [7] S. Skorik and H. Saleur, *Boundary bound states and boundary bootstrap in the sine-Gordon model with Dirichlet boundary conditions*, J. Phys. **A28** (1995) 6605–6622, preprint [hep-th/9502011](#)
- [8] P. Dorey, R. Tateo and G.M.T. Watts, *Generalisations of the Coleman-Thun mechanism and boundary reflection factors*, Phys. Lett. **B448** (1999) 249–256, preprint [hep-th/9810098](#)
- [9] A.B. Zamolodchikov and Al.B. Zamolodchikov, *Factorized S-matrices in two dimensions as the exact solutions of certain relativistic quantum field theory models*, Ann. Phys. **120** (1979) 253–291
- [10] L. Takhtadjan and L. Faddeev, Theor. Math. Phys. **21** (1974) 160  
V. Korepin and L. Faddeev, Theor. Math. Phys. **25** (1975) 147
- [11] M. Pillin, *Exact two-particle matrix elements in S-matrix preserving deformation of integrable QFTs*, Phys. Lett. **B448** (1999) 227–233, preprint [hep-th/9812106](#)
- [12] E.W. Barnes, *The Theory of the Double Gamma Function*, Phil. Trans. Roy. Soc. **A196** (1901) 265–387  
*On the Theory of the Double Gamma Function*, Trans. Cambridge Phil. Soc. **19** (1904) 376–425
- [13] M. Jimbo and T. Miwa, *QKZ equation with  $|q| = 1$  and correlation functions of the XXZ model in the gapless regime*, J. Phys. **A29** (1996) 2923–2958, preprint [hep-th/9601135](#)
- [14] A. Fring and R. Köberle, *Factorized Scattering in the Presence of Reflecting Boundaries*, Nucl. Phys. **B421** (1994) 159–172, preprint [hep-th/9304141](#)
- [15] S. Coleman and H.J. Thun, *On the Prosaic Origin of the Double Poles in the Sine-Gordon S-matrix*, Comm. Math. Phys. **61** (1978) 31
- [16] P. Christe and G. Mussardo, *Elastic S-matrices in (1+1) dimensions and Toda field theories*, Int. J. Mod. Phys. **A5** (1990) 4581–4627
- [17] H.W. Braden, E. Corrigan, P.E. Dorey and R. Sasaki, *Affine Toda field theory and exact S-matrices*, Nucl. Phys. **B338** (1990) 689–746
- [18] H.W. Braden, E. Corrigan, P.E. Dorey and R. Sasaki, *Multiple poles and other features of Affine Toda Field Theory*, Nucl. Phys. **B356** (1991) 469–498
- [19] G.W. Delius, M.T. Grisaru, and D. Zanon, *Exact S-matrices for Nonsimply-Laced Affine Toda Theories*, Nucl. Phys. **B382** (1992) 365–408, preprint [hep-th/9201067](#)
- [20] E. Corrigan, P.E. Dorey and R. Sasaki, *On a Generalised Bootstrap Principle*, Nucl. Phys. **B408** (1993) 579–599, preprint [hep-th/9304065](#)
- [21] P. Dorey, *Exact S-matrices*, in the proceedings of the 1996 Eötvös Graduate School, preprint [hep-th/9810026](#)
- [22] P. Dorey, A. Pocklington, R. Tateo and G.M.T. Watts, *TBA and TCSA with boundaries and excited states*, Nucl. Phys. **B525** (1998) 641–663, preprint [hep-th/9712197](#)
- [23] G.W. Delius and G.M. Gandenberger, *Particle reflection amplitudes in  $a_n^{(1)}$  Toda field theories*, Nucl. Phys. **B554** (1999) 325–364, preprint [hep-th/9904002](#)